



HAL
open science

Flow exchanges in multi-reservoir systems with spillbacks

Guilhem Mariotte, Ludovic Leclercq

► **To cite this version:**

Guilhem Mariotte, Ludovic Leclercq. Flow exchanges in multi-reservoir systems with spillbacks. *Transportation Research Part B: Methodological*, 2019, 122, pp.327-349. 10.1016/j.trb.2019.02.014 . hal-02068069

HAL Id: hal-02068069

<https://hal.science/hal-02068069v1>

Submitted on 14 Mar 2019

HAL is a multi-disciplinary open access archive for the deposit and dissemination of scientific research documents, whether they are published or not. The documents may come from teaching and research institutions in France or abroad, or from public or private research centers.

L'archive ouverte pluridisciplinaire **HAL**, est destinée au dépôt et à la diffusion de documents scientifiques de niveau recherche, publiés ou non, émanant des établissements d'enseignement et de recherche français ou étrangers, des laboratoires publics ou privés.



Flow exchanges in multi-reservoir systems with spillbacks

Guilhem Mariotte*, Ludovic Leclercq

Univ. Lyon, ENTPE, IFSTTAR, LICIT, Lyon, F-69518, France



ARTICLE INFO

Article history:

Received 22 December 2017

Revised 19 February 2019

Accepted 25 February 2019

Keywords:

Macroscopic fundamental diagram

Multi-reservoir systems

Congestion propagation

Trip lengths

Network traffic

Accumulation-based model

Trip-based model

ABSTRACT

Large-scale traffic flow models based on the Network Macroscopic Fundamental Diagram (MFD) are usually grounded on the bathtub analogy and a conservation equation for vehicle accumulation inside a given urban area. Recent studies have proposed a different approach where the MFD defines the spatial mean speed that is shared by all vehicles in a region while their traveling distance is tracked individually. The former approach is also referred to as “accumulation-based” while the latter is usually named “trip-based”. While extensive studies of both model properties have been carried out for the single reservoir case (a unique region), the multi-reservoir setting still requires some research effort in particular to clearly understand how inflow merge at a reservoir entry and outflow diverge at exit should be managed. These two components play a significant role in the evolution of the whole system, when flows are exchanged between multiple reservoirs. One of the crucial questions is to ensure that congestion properly propagates backwards through a succession of reservoirs when oversaturated situations are observed.

In this paper, we propose a thorough analysis of how to handle congestion propagation in the accumulation-based framework with several trip lengths or categories, e.g. internal and external trips. This allows to derive a congestion propagation model for the trip-based approach in a multi-reservoir setting. Based on theoretical considerations and simulation studies, we develop a consistent framework to restrict the inflow and adapt to oversaturated traffic conditions in a reservoir including several trip lengths. Two inflow merging schemes are investigated. The first one is inspired from the existing literature and shares the available supply based on the demand flow ratio at the entry boundary. It is called “exogenous” in contrast to the second “endogenous” scheme, which shares the supply with respect to the internal accumulation ratio on the different routes. At the reservoir exit, a new outflow diverging scheme is also introduced to better reproduce the effect of queuing vehicles that are prevented from exiting the reservoir when congestion spills back from neighboring reservoirs. Compared to the conventional outflow model, our new approach proves to avoid unrealistic gridlocks when the reservoir becomes oversaturated. Both entry and exit flow models are investigated in details considering the accumulation-based and trip-based frameworks. Finally, the most consistent approach is compared with two other existing MFD models for multiple reservoirs. This demonstrates the importance of properly handling entry and exit flows at boundaries.

© 2019 The Authors. Published by Elsevier Ltd.
This is an open access article under the CC BY-NC-ND license.
(<http://creativecommons.org/licenses/by-nc-nd/4.0/>)

* Corresponding author.

E-mail address: guilhem.mariotte@ifsttar.fr (G. Mariotte).

1. Introduction

Over the past decade, the Macroscopic Fundamental Diagram (MFD) has appeared to be a powerful tool to describe traffic states at the network level with few implementation and computational efforts. Many studies have notably used MFD-based traffic simulators for several promising applications, like traffic state estimation (where contributions can be found in [Knoop and Hoogendoorn, 2014](#); [Yildirimoglu and Geroliminis, 2014](#)), perimeter control ([Keyvan-Ekbatani et al., 2012](#); [Haddad, 2015](#); [Haddad and Mirkin, 2017](#); [Ampountolas et al., 2017](#)), route guidance at large scale ([Hajiahmadi et al., 2013](#); [Yildirimoglu et al., 2015](#); [Ding et al., 2017](#)), or analyzing cruising-for-parking issues ([Leclercq et al., 2017](#); [Cao and Menendez, 2015](#); [Zheng and Geroliminis, 2016](#)). Their modeling approaches take advantage of the multi-reservoir representation of a city, where the dynamics of each urban reservoir (sometimes also called “neighborhood”, “zone” or “region”) is described by the single reservoir model of [Daganzo \(2007\)](#). This framework, also referred as the “accumulation-based” model, assumes that the reservoir outflow is proportional to the total circulating flow inside the zone if one consider a constant average trip length assigned to all travelers. Some authors have extended this approach to account for multiple trip lengths in a reservoir, either to develop new applications like modeling search-for-parking ([Geroliminis, 2009](#); [2015](#)) and macroscopic routing (with contributions in [Yildirimoglu et al., 2015](#); [Ramezani et al., 2015](#)); or to highlight inaccuracies in MFD-based models due to the constant trip length hypothesis ([Yildirimoglu and Geroliminis, 2014](#); [Leclercq et al., 2015](#)). More recently, a “trip-based” formulation of the single reservoir model has gained a new interest in the community. Based on an idea of [Arnott \(2013\)](#), this approach has been exploited in [Daganzo and Lehe \(2015\)](#) and then [Lamotte and Geroliminis \(2018\)](#), [Mariotte et al. \(2017\)](#) and [Leclercq et al. \(2017\)](#). The principle is that all users in a reservoir share the same space-mean speed (given by the MFD) at a given time, and exit once they have completed their individually assigned trip length. As shown in a thorough comparison with the accumulation-based model by [Mariotte et al. \(2017\)](#), the trip-based approach gives more accurate results during transient phases, especially in terms of experienced travel time. Nevertheless, some authors like [Haddad and Mirkin \(2016\)](#) and [Haddad and Zheng \(2017\)](#) suggest that the inaccuracies of the accumulation-based model can be taken into account directly by implementing delays either in the control inputs or in the state of the dynamic system. A proper investigation about the properties of these new modeling approaches is still missing, in particular to assess their differences with the trip-based model. While we choose to focus on the accumulation-based and trip-based models in this paper, integrating these new approaches could be interesting for further research directions.

However, from the modeler’s perspective, despite all these recent advances in MFD-based simulation, congestion propagation in a multi-reservoir framework is not fully understood yet. Notably, the questions of if and how boundary flows should be limited when a reservoir is oversaturated, and how to distribute inflows and outflows have not been completely addressed. In details, as the wide majority of MFD-based simulators are developed for control applications, most authors argue, with reason, that the controllers will not allow the reservoir to reach highly congested states, so that the aforementioned concerns may be eclipsed in their traffic flow models (see e.g. [Kouvelas et al., 2017](#)). However, other applications of MFD-based models should not ignore them. Actually some interesting works already propose incomplete but viable solutions to deal with congestion propagation. [Hajiahmadi et al. \(2013\)](#) and [Lentzakis et al. \(2016\)](#), whose simulator is based on the Network Transmission Model (NTM) of [Knoop and Hoogendoorn \(2014\)](#), consider exogenous boundary capacities between reservoirs and a global entry supply function per reservoir, similar to the Cell Transmission Model (CTM) of [Daganzo \(1994\)](#). Their approach ensures a perfect protection of the reservoirs from global gridlock, nevertheless this one can hardly be extended to heterogeneous trip lengths within reservoirs. [Yildirimoglu and Geroliminis \(2014\)](#) certainly developed the most advanced tool in MFD-based simulation, as they account for different trip lengths and manage flow exchanges with a Dynamic Traffic Assignment (DTA) procedure on macroscopic routes (a route being a succession of reservoirs, sometimes called a regional path). Their framework served as a basis for recent and promising large-scale control schemes ([Ramezani et al., 2015](#); [Yildirimoglu et al., 2015](#); [Sirmatel and Geroliminis, 2017](#); [Yildirimoglu et al., 2018](#)). However, they handle each boundary between two adjacent reservoirs separately with a demand pro-rata inflow merge, and do not provide any further information about the consistency of the global traffic dynamics when some reservoirs are oversaturated.

The main objective of this study is to properly address congestion spillback in multi-reservoir systems. Our contribution is to identify, analyze and eventually modify the critical components of MFD-based models to build up a consistent simulation framework in both under- and oversaturation. In particular, we will ensure that flow exchanges at interfaces are fulfilling the main assumptions of MFD-based modeling (traffic state homogeneity) and the classical principles of kinematic wave theory (flow conservation, supply limitation, etc). For the accumulation-based model, we will refer to the framework of [Yildirimoglu and Geroliminis \(2014\)](#) and [Geroliminis \(2015\)](#). For the trip-based model, we will pursue the effort of [Mariotte et al. \(2017\)](#) who provide a first attempt to handle spillbacks in this formulation. We notably extend and propose new inflow and outflow modeling approaches that prove to overcome some shortcomings we noticed about the conventional models from the literature. This study focuses on methodological contributions and aims to provide a thorough description of how traffic dynamics in reservoirs are influenced by the model design. In parallel, the authors are working on designing specific test cases using microscopic simulation to validate the proposed approaches. The results will be presented in a different paper.

This paper is organized as follows. [Section 2](#) presents the case of a single reservoir with a unique trip length. This section allows to set the background of our study and its assumptions, and also discusses and proposes an efficient method to account for spillbacks in the trip-based approach. [Section 3](#) deals with inflow and outflow allocation between multiple trip categories in one reservoir, especially when congestion propagates through the reservoir. Numerical examples are then given

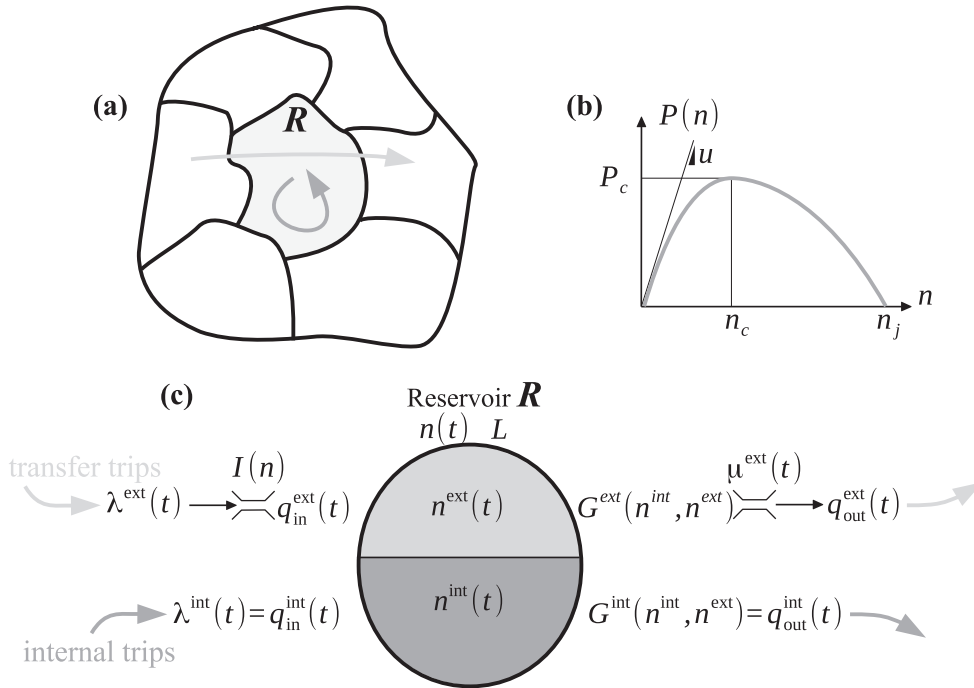


Fig. 1. (a) Representation of the single reservoir in a multi-reservoir context, (b) typical production-MFD for the reservoir, and (c) representation of flow modeling for the two trip category, transfer trips and internal trips.

in Section 4 for a single reservoir crossed by two trip categories. Finally, Section 5 illustrates the differences in simulation between a new approach we proposed and two existing models from the literature for a multi-reservoir system.

2. Flow transfer in a single reservoir with a unique trip length

2.1. Accumulation-based modeling

In this section, we focus on the interactions between one reservoir and its neighbors in the context of a multi-reservoir representation of a city, as represented in Fig. 1(a).

The concept of the single reservoir model has been first presented in Daganzo (2007) and Geroliminis and Daganzo (2007). It corresponds to a selection of connected links and nodes of an urban network where traffic states are characterized by a well-defined production-MFD $P(n)$ (in [veh.m/s]), or equivalently, a speed-MFD $V(n) = P(n)/n$ (in [m/s]), where n (in [veh]) is the total accumulation (number of circulating vehicles in the reservoir). The production-MFD is defined through its jam accumulation n_j , critical accumulation n_c at which the maximum production or capacity is reached: $P_c = P(n_c)$ and free-flow speed u , see Fig. 1(b). The reservoir entry border (also conceptually called “upstream boundary”) gathers all individual entry nodes of the network; similarly the reservoir exit border (or “downstream boundary”) contains all the exit nodes. Because our focus is on flow exchanges between different reservoirs in a multi-reservoir context, for the single reservoir model we will distinguish between “external” and “internal” origin/destination of trips. A trip with an external origin (resp. destination) crosses the entry (resp. exit) border, whereas a trip with an internal origin (resp. destination) originates (resp. ends) inside the reservoir. A lot of studies dealing with MFD-based aggregated dynamics do the distinction between “internal” trips, i.e. originating and ending inside the reservoir, and “transfer” trips, i.e. crossing the reservoir from the entry to the exit border. However they are often handled by the same modeling approach, so that a proper definition of inflow and outflow is somehow missing. In control-oriented works, some authors like Aboudolas and Geroliminis (2013), Ampountolas et al. (2017) and Kouvelas et al. (2017) split the inflow into the receiving flow from adjacent reservoirs (for which the controllers apply), and the “uncontrolled demand” which may be from inside or outside. In this section, we propose a consistent modeling approaches for a single reservoir with transfer trips and internal trips.

2.1.1. Traffic dynamics

In a reservoir, traffic dynamics are essentially described by the conservation of vehicles, first mentioned in Daganzo (2007) for a unique trip category and extended to multiple trip categories by Geroliminis (2009, 2015). The

conservation equations of a single reservoir with a transfer trip category and an internal trip category are as follows:

$$\begin{cases} \frac{dn^{\text{ext}}}{dt} = q_{\text{in}}^{\text{ext}}(t) - q_{\text{out}}^{\text{ext}}(t) \\ \frac{dn^{\text{int}}}{dt} = q_{\text{in}}^{\text{int}}(t) - q_{\text{out}}^{\text{int}}(t) \end{cases} \quad (\text{reservoir dynamics}) \quad (1)$$

where $n^{\text{ext}}(t)$, $q_{\text{in}}^{\text{ext}}(t)$ and $q_{\text{out}}^{\text{ext}}(t)$ are respectively the accumulation, the inflow and outflow of the transfer trips; and $n^{\text{int}}(t)$, $q_{\text{in}}^{\text{int}}(t)$ and $q_{\text{out}}^{\text{int}}(t)$ are respectively the accumulation, the inflow and outflow of the internal trips. By definition, $n(t) = n^{\text{ext}}(t) + n^{\text{int}}(t)$ is the total accumulation. The reservoir model and its boundary conditions are represented in Fig. 1(c). Because the transfer trips cross the reservoir borders, they may experience flow restrictions due to the interactions with neighboring reservoirs (capacity or speed reduction due to traffic conditions in the reservoirs). At entry, the effective inflow $q_{\text{in}}^{\text{ext}}(t)$ is thus the minimum between its upstream demand $\lambda^{\text{ext}}(t)$ and an endogenous limitation $I(n(t))$. The latter function aims at reproducing congestion spilling back to the reservoir entry in oversaturation, it is usually called the “entry supply function” (or sometimes the “receiving capacity”). Its existence and shape are discussed in the following subsection. If the demand for internal trips remains quite low compared to the MFD capacity, it is reasonable to assume that these trips do not experience any delay in departure time inside the reservoir. This is also discussed in the following. In this case the effective inflow $q_{\text{in}}^{\text{int}}(t)$ equals its demand $\lambda^{\text{int}}(t)$. In short, we have:

$$\begin{cases} q_{\text{in}}^{\text{ext}}(t) = \min[\lambda^{\text{ext}}(t); I(n(t))] \\ q_{\text{in}}^{\text{int}}(t) = \lambda^{\text{int}}(t) \end{cases} \quad (\text{effective inflows}) \quad (2)$$

Note that in this framework, the accumulation of vehicles waiting for entering the reservoir in case of an inflow restriction is taken into account with a point-queue model at entry. Hence the upstream demand $\lambda^{\text{ext}}(t)$ is set to a maximum—for instance, the maximum of $I(n)$ —every time that this queue is not empty.

At exit, the system potential outflow is determined by the reservoir internal dynamics, which are described either by the accumulation-based model or the trip-based model. We investigate here the accumulation-based model first. In its simplest version, a unique trip length L (in [m]) is considered for all the travelers. By applying the queuing formula of Little (1961), the total potential outflow $G(n)$ (in [veh/s]), also called “trip completion rate”, is defined as $G(n) = n/L \cdot V(n) = P(n)/L$ (Daganzo, 2007). $G(n)$ is thus also named the outflow-MFD (Lamotte and Geroliminis, 2018). This quasi-static approach has several limitations as detailed in Mariotte et al. (2017). According to Geroliminis and Daganzo (2007) and Geroliminis (2009), the potential outflow of each trip category is calculated with its ratio of partial accumulation over the total accumulation, which is also an application of Little’s formula:

$$\begin{cases} G^{\text{ext}}(n^{\text{int}}, n^{\text{ext}}) = \frac{n^{\text{ext}}}{n} G(n) = \frac{n^{\text{ext}}}{n} \frac{P(n)}{L} \\ G^{\text{int}}(n^{\text{int}}, n^{\text{ext}}) = \frac{n^{\text{int}}}{n} G(n) = \frac{n^{\text{int}}}{n} \frac{P(n)}{L} \end{cases} \quad (\text{trip completion rate}) \quad (3)$$

Here again, because the transfer trips may experience a flow limitation when entering the next reservoir at downstream, the effective outflow $q_{\text{out}}^{\text{ext}}(t)$ is the minimum between its outflow demand $G^{\text{ext}}(n^{\text{int}}(t), n^{\text{ext}}(t))$ and an exogenous restriction $\mu^{\text{ext}}(t)$. The internal trips can reach their destinations according to their potential outflow definition without any additional restriction. Thus we have:

$$\begin{cases} q_{\text{out}}^{\text{ext}}(t) = \min[\mu^{\text{ext}}(t); G^{\text{ext}}(n^{\text{int}}(t), n^{\text{ext}}(t))] \\ q_{\text{out}}^{\text{int}}(t) = G^{\text{int}}(n^{\text{int}}(t), n^{\text{ext}}(t)) \end{cases} \quad (\text{effective outflows}) \quad (4)$$

While being satisfying for the outflow model of internal trips, the current definition of the outflow demand $G^{\text{ext}}(n^{\text{int}}, n^{\text{ext}})$ for the transfer trips has some critical shortcomings that are discussed later in Section 2.1.3.

2.1.2. The entry supply function

When the reservoir is oversaturated, the entry supply function $I(n)$ dynamically restricts the incoming flow to mimic the propagation of congestion inside the reservoir.¹ Its general shape is thus a decreasing function of the total accumulation n . Its existence was first noticed in Geroliminis and Daganzo (2007) with simulation loadings on the network of downtown San Francisco, USA. Then, authors like Ramezani et al. (2015) and Sirmatel and Geroliminis (2017) used theoretical piecewise linear decreasing functions to avoid creating gridlocks in their multi-reservoir modeling. These functions were rather implemented for practical reasons because the authors provided few details about how to design them. Kouvelas et al. (2017) mentioned that the entry supply function is not always required: it can be ignored for a reservoir that remains undersaturated or which is protected by a perimeter control system. In the general case, i.e. without such a protection, a reservoir can go to gridlock when loaded with an inflow demand higher than its MFD flow capacity P_c/L , as highlighted by Laval et al. (2018). Because the outflow follows the evolution of $G(n)$ by definition, it cannot sustain an equilibrium flow higher than P_c/L . Then, an effective way to protect the reservoir may be to adopt a shape of $I(n)$ similar to the supply function of the CTM: $I(n) = P_c/L$ if $n \leq n_c$ and $I(n) = G(n)$ otherwise. This was notably the choice of Hajiahmadi et al. (2013), Knoop and Hoogendoorn (2014) and Lentzakis et al. (2016). Nevertheless, this approach is clearly too restrictive in MFD

¹ Used along the whole paper, this notion of propagation actually means the evolution of traffic states towards oversaturation, i.e. the increase of accumulation above n_c , as there is no spatial variable in a reservoir, only a time variable.

simulation as it prevents any inflow surge from entering the reservoir. If this were true, the inflow would be always auto-regulated and there would be no need for perimeter control at all. Actually, P_c/L corresponds to the reservoir capacity in a stationary state. When this capacity is driven by internal bottlenecks in the middle of the reservoir, it would not be surprising to observe higher inflow values during a network loading before all these bottlenecks are activated and make the congestion spilling back to the perimeter. The choice of the critical accumulation n_c to distinguish under- and oversaturated conditions in $I(n)$ is also a matter of debate. Unlike the above-mentioned studies, Geroliminis and Daganzo (2007) found with simulation results that the critical accumulation of $I(n)$ may be higher than n_c .

Based on these approaches from the literature, we further investigate the shape of the entry supply function here. In the most general case, the inflow willing to enter a given reservoir may be first limited by a physical constraint, which is the sum of the capacities of all the links that define the reservoir entry border. This idea of a fixed capacity assigned to a reservoir border was also mentioned in Knoop and Hoogendoorn (2014) and Ramezani et al. (2015). Let us consider the simple case of a single entry border first, in this situation the maximum of $I(n)$ precisely corresponds to this physical constraint, which applies for low accumulations (undersaturation). Then, above some critical accumulation, the limiting factor becomes the reservoir inner state which undergoes saturation or oversaturation: the higher the accumulation, the lesser the total inflow. How the inflow limitation should be close to the reservoir saturation is still unclear, but it is obvious that this limitation should exactly follows the outflow-MFD $G(n)$ at some point to ensure a consistent flow equilibrium in the system. It is worth noticing that this notion of equilibrium also describes the transient state of the system, because of the underlying quasi-static hypothesis in the accumulation-based model. Moreover, the inflow limitation should be consistent with the outflow when internal trips are considered as well. Under our assumption that a low demand for internal trips is unrestricted, the effective limitation that applies to the transfer trips is therefore $I(n(t)) - \lambda^{\text{int}}(t)$. This approach should be reasonable when the demand $\lambda^{\text{int}}(t)$ remains low and evolves slowly with time. But this is probably not the case for high and fast-varying peaks for internal trips, as this would mean high and instantaneous changes in the available inflow supply for transfer trips, just as if the reservoir internal dynamics would instantaneously adapt to a demand surge of internal trips. Then, a better way to handle these trips is to restrict their inflow similarly to transfer trips, by using either the same entry supply function or a different function for internal trips. A merging scheme could be also used to allocate the right limitation to each trip category, but this falls into the framework of multiple trip lengths in the single reservoir model, which is investigated later in Section 3.

To illustrate the application of the entry supply function, we simulate several network loadings in a single reservoir with the characteristics: $n_j = 1000$ veh, $n_c = 400$ veh, $P_c = 3000$ veh.m/s, $L = 2.5$ km and $u = 15$ m/s. The reservoir includes internal trips with a low constant demand of $\lambda^{\text{int}}(t) = 0.3$ veh/s, and transfer trips with demand levels ranging from $\lambda^{\text{ext}}(t) = 0.8$ to 1.3 veh/s. The reservoir total flow capacity equals $P_c/L = 1.2$ veh/s, which means that at some points the total inflow demand will exceed this capacity. Fig. 2 presents the simulation results in the total accumulation - total inflow plane ($n(t)$, $q_{\text{in}}(t)$) for three different function models of $I(n)$. Model 1 corresponds to the model adopted by Knoop and Hoogendoorn (2014) with a higher limit in undersaturation. In this example this limit is arbitrary set to 1.7 veh/s, but this value should come from the aggregation of all entering link capacities in a real situation. Model 2 is similar to model 1 except that its critical accumulation n_{cs} is higher than n_c . Finally, model 3 does not match the outflow-MFD $G(n)$ at all and allows higher inflows to enter the reservoir. Fig. 2(a)–(c) consist of a demand surge while Fig. 2(d)–(f) present the same simulations with a peak demand profile: the high demand level is kept for a much shorter period in this case. This simple example allows us to exhibit obvious drawbacks of some models. While potentially allowing high inflows in undersaturation, model 1 is not satisfying because the accumulation cannot exceed n_c which is too restrictive compared to what we may observe in reality, see Fig. 2(a) and (d). Actually, we know from empirical data that a network can reach oversaturated states while being loaded with both transfer and internal trips (Geroliminis and Daganzo, 2008). As shown in Fig. 2(f), model 3 can effectively reproduce reliable network loading and unloading with the demand peak profiles. However, it is unable to protect the reservoir from gridlock if a high level of demand above the MFD capacity is maintained during a longer period, see also Fig. 2(c). In this case, apart from setting a maximum inflow limit, the entry supply function does not seem of great utility. Model 2 is certainly the best compromise between model 1 and model 3, and proves to reproduce reliable traffic state evolutions in all demand settings as shown in Fig. 2(b) and (e). This illustrates that at some point in oversaturation $I(n)$ must be confounded with $G(n)$ to stabilize the system and avoid a fast unrealistic attraction to gridlock in many situations. Interestingly, the use of a shape of $I(n)$ similar to model 2 implies that there is a theoretical maximum accumulation n_{cs} that cannot be exceeded when loading a network, which is precisely the critical accumulation of $I(n)$. Further empirical studies or comparisons with microsimulation are needed to validate this property, as well as the shape of $I(n)$ ensuring the transition between under- and oversaturated states. Such validations are part of further research and out of the scope of our theoretical considerations developed in this paper.

2.1.3. Modeling exit rate for transfer trips

We now discuss the description of vehicles exiting the reservoir and propose a new outflow model for transfer trips. To our best knowledge, all the studies from the literature consider that the system total demand for outflow (or total effective outflow if they do not apply supply limitations) always equals $G(n)$. In our opinion however, we believe that this is only true to model internal congestion for the outflow of internal trips $G^{\text{int}}(n^{\text{int}}, n^{\text{ext}})$, but that a distinction between what we call the exit demand function $O^{\text{ext}}(n^{\text{int}}, n^{\text{ext}})$ and $G^{\text{ext}}(n^{\text{int}}, n^{\text{ext}})$ should be made for transfer trips. Note that $O^{\text{ext}}(n^{\text{int}}, n^{\text{ext}})$ is not the effective outflow $q_{\text{out}}^{\text{ext}}(t)$, which is the result of the competition between demand and supply as written in

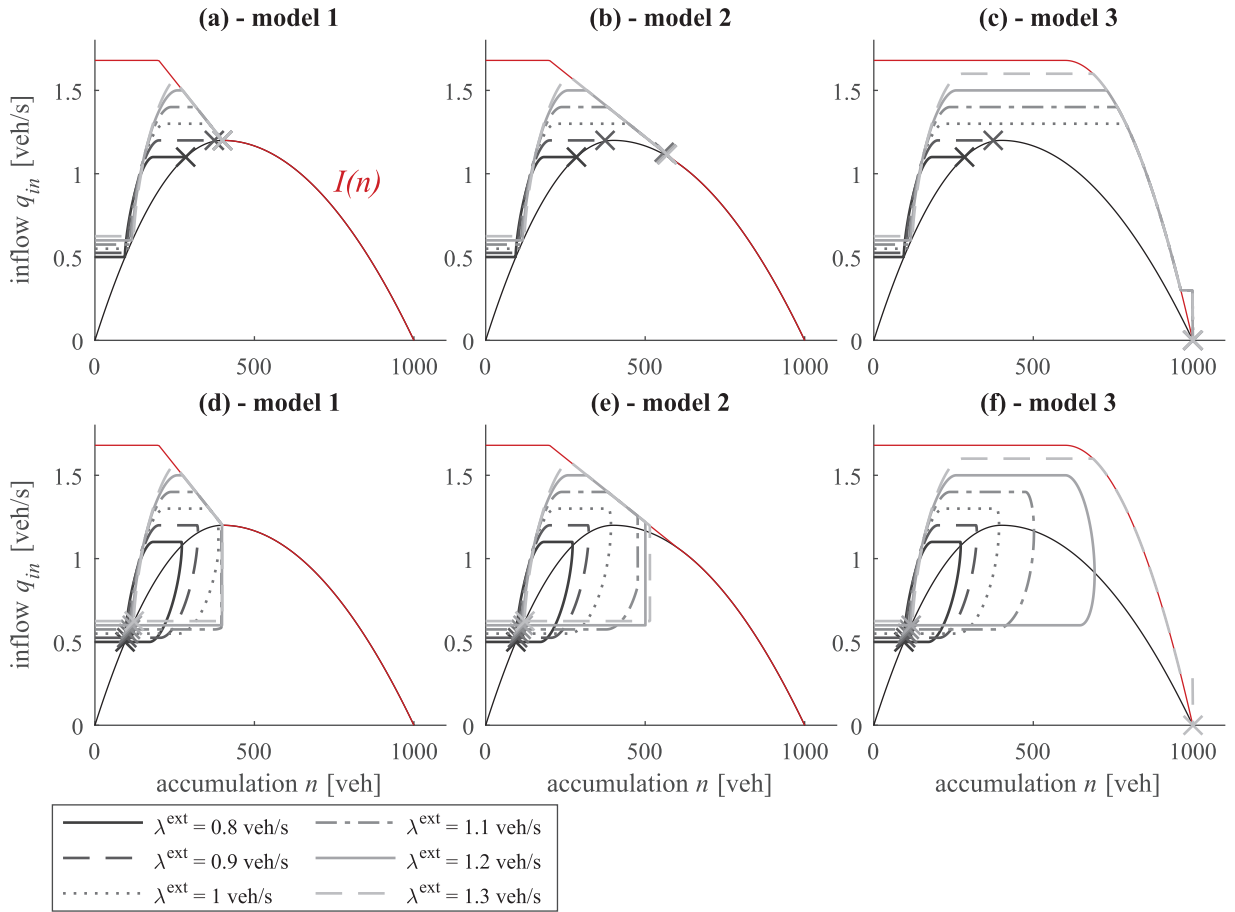


Fig. 2. Network loading of the single reservoir with transfer and internal trips for different shapes of the entry supply function. (a) Demand surge for transfer trips with entry supply model 1, (b) model 2 and (c) model 3. (d) Demand peak for transfer trips with entry supply model 1, (e) model 2 and (f) model 3. The legend indicates the demand value for the gap or the peak.

Eq. (6). With the traditional approach, the reservoir can easily converge to heavily congested situations without any possibility to recover, even if the next reservoirs have plenty of capacity left. This phenomenon was notably highlighted by Mariotte et al. (2017) with a supply reduction scenario at exit. This issue happens only if $O^{ext}(n^{int}, n^{ext})$ describes the demand for outflow and not the effective outflow. In classical kinematic wave theory, the observed flow at the head of a queue is always equal to the available capacity. This is mathematically expressed by a demand value equal to the maximal capacity for saturated and oversaturated regimes. We should observe the same behavior when a reservoir is discharging without external downstream constraints. If $O^{ext}(n^{int}, n^{ext})$ always equals $G^{ext}(n^{int}, n^{ext})$ for $n > n_c$, the outflow demand is very low for a high accumulation n as congestion spills back from a downstream reservoir (represented by the exogenous limitation μ^{ext}). The consequence of this low outflow is that the queue cannot empty when congestion disappears from the downstream reservoir (i.e. when μ^{ext} is removed). This even leads to an increase of accumulation and thus a lower outflow and so on until the system stabilizes once inflow equals outflow. At this point, the reservoir cannot retrieve a free-flow situation, even though the downstream constraint does not exist anymore. This can be avoided if we adopt the following definition of outflow demand for transfer trips:

$$O^{ext}(n^{int}, n^{ext}) = \begin{cases} \frac{n^{ext}}{n} \frac{P(n)}{L} = G^{ext}(n^{int}, n^{ext}) & \text{if } n < n_c \\ \frac{n^{ext}}{n} \frac{P_c}{L} & \text{otherwise} \end{cases} \quad (\text{exit demand function}) \quad (5)$$

Hence the new model of outflow for the single reservoir with transfer and internal trips becomes:

$$\begin{cases} q_{out}^{ext}(t) = \min[\mu^{ext}(t); O^{ext}(n^{int}(t), n^{ext}(t))] \\ q_{out}^{int}(t) = G^{int}(n^{int}(t), n^{ext}(t)) \end{cases} \quad (\text{effective outflows}) \quad (6)$$

The idea behind the expression in Eq. (5) is that the potential outflow of transfer trips is now constant and independent from the reservoir state in oversaturation ($n > n_c$). This mimics the behavior of users that are physically queuing at the exit of the network to enter a neighboring reservoir, similarly to the description of cell outflow in the CTM. In case of a reservoir

defined by its MFD, the maximum rate at which users can exit the network is given by the reservoir capacity or maximum throughput P_c/L . Without having access to the ground truth, we cannot claim that the latter expression is more or less realistic than the traditional approach $O^{\text{ext}}(n^{\text{int}}, n^{\text{ext}}) = G^{\text{ext}}(n^{\text{int}}, n^{\text{ext}})$. Nevertheless, our proposition is specifically designed to handle flow exchanges during congestion periods in multi-reservoir systems, according to what is already well-known in link-scale traffic flow theory. Because temporarily supply limitations are very likely to occur at the reservoir perimeter when congestion propagates, assuming $O^{\text{ext}}(n^{\text{int}}, n^{\text{ext}}) = G^{\text{ext}}(n^{\text{int}}, n^{\text{ext}})$ would often lead to gridlock, making such a model quite useless in practice to study oversaturated situations over a large-time horizon. The traditional approach is actually based on observations from either simulation studies (Geroliminis and Daganzo, 2007) or empirical evidences (Geroliminis and Daganzo, 2008), but what these authors observed is the effective outflow. Whereas our modeling framework is based on the demand for outflow, a quantity which is not measurable in simulation nor in real field. This concept proves to be efficient to avoid the extreme situation mentioned above and illustrated further in Section 2.3 when considering transfer trips only.

2.2. Trip-based modeling

We now focus on the modeling of spillbacks in the trip-based approach. The theoretical background of the trip-based model has been first introduced by Arnott (2013). Let us consider a single reservoir with a unique trip length L . In a first step, we only consider transfer trips in the trip-based model, so that $n = n^{\text{ext}}$, because the formulation of this approach is much more complex than the accumulation-based one. The general case with multiple trips for both accumulation- and trip-based models will be presented in Section 3. At each time t , all the vehicles are traveling at the same speed $V(n(t))$. A user exiting the reservoir at t has experienced a travel time of $T(t)$. This user thus entered the reservoir at $t - T(t)$, and his/her trip distance was L . The trip-based model considers that the accumulation and therefore the mean speed may change during the user's trip, which is mathematically expressed as:

$$L = \int_{t-T(t)}^t V(n(s)) ds \quad (7)$$

By using basic relationships based on entering and exiting count curves, it can be shown that the derivative of Eq. (7) leads to (see e.g. Arnott, 2013; Mariotte et al., 2017):

$$q_{\text{out}}(t) = q_{\text{in}}(t - T(t)) \cdot \frac{V(n(t))}{V(n(t - T(t)))} \quad (8)$$

Using Eq. (8) to solve the conservation Eq. (1) either for internal or transfer trips leads to a differential equation with endogenous delay. Despite being mathematically intractable, this formulation of the outflow can allow the development of efficient numerical resolution schemes (continuous approximation on vehicle indexes or event-based resolution method), as shown in Mariotte et al. (2017). A simpler formulation integrating static delays has been proposed for the accumulation-based model by Haddad and Zheng (2017). However, a comparison study is currently missing to assess the differences between these both approaches, so that in this paper we decided to focus on the more refined trip-based formulation. These resolution methods of the latter work in free-flow only, where $q_{\text{in}}(t)$ is the input, equal to the inflow demand $\lambda(t)$, and where $q_{\text{out}}(t)$ is the consequence of the system evolution. In congestion however, the role of inflow and outflow are switched, as $q_{\text{out}}(t)$ becomes the given boundary condition, equal to the outflow supply $\mu(t)$, and $q_{\text{in}}(t)$ has now to adapt to the system evolution due to the restriction at exit. It can be shown that Eq. (8) can be reversed to express $q_{\text{in}}(t)$ as a function of $q_{\text{out}}(t)$:

$$q_{\text{in}}(t) = q_{\text{out}}(t + T^*(t)) \cdot \frac{V(n(t))}{V(n(t + T^*(t)))} \quad (9)$$

where $T^*(t)$ is the exact predictive travel time, i.e. the time during which the user entering at t will travel, see also Fig. 3. By construction we have: $T(t) = T^*(t - T(t))$. But Eq. (9) means that to calculate the effect of an exit flow limitation on the entry, one needs to know the future of the system, which is problematic. First, it is not possible to deduce the inflow when downstream supply restriction should apply, and second, if this was possible we have no clue on how to make the switch.

Thus in practice, this model needs to be coupled with another model for reproducing congestion propagation. A first attempt has been made by Mariotte et al. (2017). They assume a free-flow evolution of the system and then apply the outflow reduction and the minimum principle of Newell (1993) on the inflow. This method with off-line calculations is sufficient for the analysis of a single reservoir, but not suitable in a multi-reservoir context where traffic states in the reservoirs depend from each other all the time. In our study, we propose a simple way to perform in-line computations, i.e. step by step, of inflow limitations in the trip-based model. It consists in switching to the accumulation-based framework in congestion, by using the same entry supply function $I(n)$ which restrains inflow for high values of accumulation n . We show in the next section with simple simulation scenarios that such a method works well in practice.

2.3. Numerical implementation

In the following of this paper, we will use the event-based scheme presented in Mariotte et al. (2017) to solve numerically the trip-based model. In congestion, the reservoir exit flow of transfer trips is limited to $\mu^{\text{ext}}(t)$ at each time by retaining

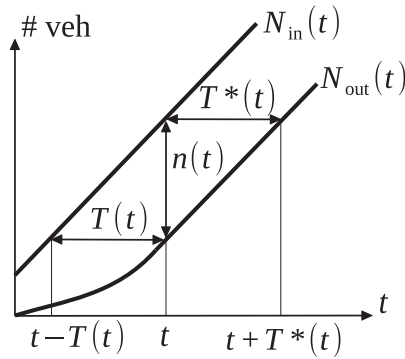


Fig. 3. Cumulative count curves of the single reservoir with the total accumulation $n(t)$, the experienced travel time $T(t)$ and the exact predictive travel time $T^*(t)$.

the vehicles inside the zone until the next exit time, even if they have already completed their trip length. At entry, the inflow limitation is ensured with the definition of a minimum or supply time for entering the reservoir:

$$t_{\text{entry supply}}^{N^{\text{in}}} = t_{\text{entry}}^{N^{\text{in}}-1} + \frac{1}{l(n)} \quad (\text{entry supply time}) \quad (10)$$

where $t_{\text{entry supply}}^{N^{\text{in}}}$ is the supply time for the N^{in} th vehicle to enter the reservoir, $t_{\text{entry}}^{N^{\text{in}}-1}$ is the entering time of the previous vehicle, and $l(n)$ is the entry supply function of the accumulation-based model introduced in Section 2.1.

The application of this method is illustrated with two test cases with transfer trips only. We have therefore: $n(t) = n^{\text{ext}}(t)$, $q_{\text{in}}(t) = q_{\text{in}}^{\text{ext}}(t)$, $q_{\text{out}}(t) = q_{\text{out}}^{\text{ext}}(t)$, $\lambda(t) = \lambda^{\text{ext}}(t)$ and $\mu(t) = \mu^{\text{ext}}(t)$. The entry supply function has a shape similar to model 1 in these examples. The first test case is about a demand peak temporarily exceeding the exit supply, and the second one concerns a supply reduction at exit below the demand level at entry. These numerical examples consider a single reservoir with the same characteristics as in Section 2.1.

Fig. 4(a1) shows the demand $\lambda(t)$ and supply $\mu(t)$ profiles for the demand peak case. The simulation scenario has been designed to let the congestion reach the entry before the demand decreases. The reservoir state evolution is presented in Fig. 4(b1) and (c1) with the inflow/outflow and accumulation. The blue curves correspond to the accumulation-based model, the green ones to the trip-based model. Note that a queue at the reservoir entry is taken into account when vehicles are waiting to enter if the inflow is limited in both models, though not presented here. All graphs show similar results for both modeling approaches. This was actually expected, since the modeling of spillbacks is handled in the same manner in both models. This also proves that the switch to the accumulation-based model works well in the trip-based framework with few modifications in the event-based resolution scheme.

Fig. 4(a2) shows the demand $\lambda(t)$ and supply $\mu(t)$ profiles for the supply reduction case. Similarly, the simulation scenario has been designed to let the congestion reach the entry before the exit supply increases again. In Fig. 4(b2) and (c2), the red and yellow curves corresponds to the evolution of inflow/outflow and accumulation when O^{ext} always equals G^{ext} as it is traditionally assumed in the literature. In the accumulation-based model (in red), we observe that the system reaches an equilibrium point once inflow equals outflow shortly after 4000 s. Then, the reservoir state does not evolve anymore because after this point the outflow corresponds to the exit demand O^{ext} , and thus $q_{\text{out}}(t)$ is not impacted by an increase of $\mu(t)$, see Eq. (6). In the trip-based approach (in yellow), the users travel at a low mean speed after 4000 s to adapt the exit supply reduction. But when this limitation disappears, the vehicle exit rate is still the same because the mean speed remains low, and consequently the system cannot recover from congestion in this framework too. We can fix this problem if we keep the outflow demand O^{ext} maximum during severe congestion periods. This can be modeled in the trip-based framework only if we force the travelers to complete their trip length at a pace that matches the exit time defined by the outflow when $n \geq n_c$. Theoretically, it implies that the related users will have a speed different from $V(n)$ during congested situations. This formulation happens to be equivalent to the outflow demand definition of Eq. (5). This is illustrated by the blue and green curves in Fig. 4(b2) and (c2), which also show similar results for both models.

3. Flow transfer in a single reservoir with multiple trip lengths

3.1. Accumulation-based framework

This section aims at extending the previous considerations on inflow and outflow modeling when a single reservoir includes multiple trip categories. This is the last step towards our final purpose: proposing a robust modeling framework for congestion propagation in a multi-reservoir environment. Like Yildirimoglu and Geroliminis (2014), we consider that users are assigned to a set of given “macroscopic routes” or sometimes called “regional paths”, defined as successions of reservoirs, as illustrated in Fig. 5(a). Following the approach of these authors, it is assumed that the system state can be described at

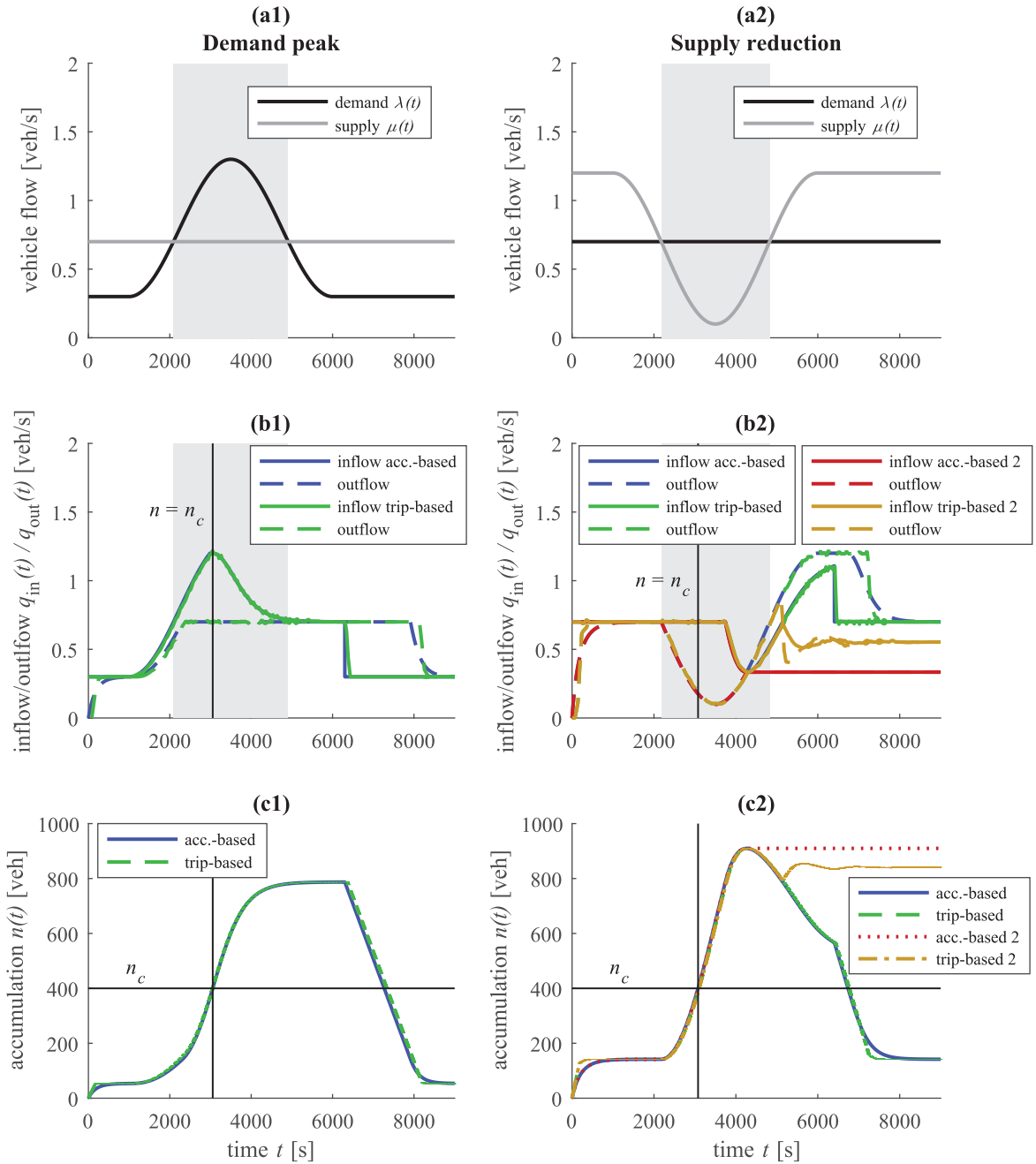


Fig. 4. (a1) Demand peak at the reservoir entry, demand $\lambda(t)$ and supply $\mu(t)$ profiles where the gray area indicates when demand exceeds supply, (b1) inflow $q_{in}(t)$ and outflow $q_{out}(t)$ and (c1) accumulation $n(t)$ for the accumulation and trip-based models. (a2) Supply reduction at the reservoir exit, demand and supply profiles where excess of demand compared to supply is indicated by the gray area, (b2) inflow and outflow and (c2) accumulation for the accumulation- and trip-based models, where model “2” corresponds to the situation when O^{ext} always equals G^{ext} . (For interpretation of the references to color in this figure legend, the reader is referred to the web version of this article.)

the level of the macroscopic routes, later simply referred to as “routes”. The reader can refer to [Batista et al. \(2019\)](#) for more details about the concept of macroscopic routes and the methods to estimate their lengths. As a reservoir can be crossed by different routes with different trip lengths, the thorough understanding of flow dynamics in one reservoir with heterogeneous trip lengths is essential to build a proper multi-reservoir simulation tool.

The extension of the single reservoir model with one trip length to several trip lengths has been first established in [Geroliminis \(2009, 2015\)](#). This theoretical framework has then been used in various studies with more complex multi-reservoir settings (e.g. [Yildirimoglu and Geroliminis, 2014](#); [Ramezani et al., 2015](#); [Yildirimoglu et al., 2018](#)). Note that the

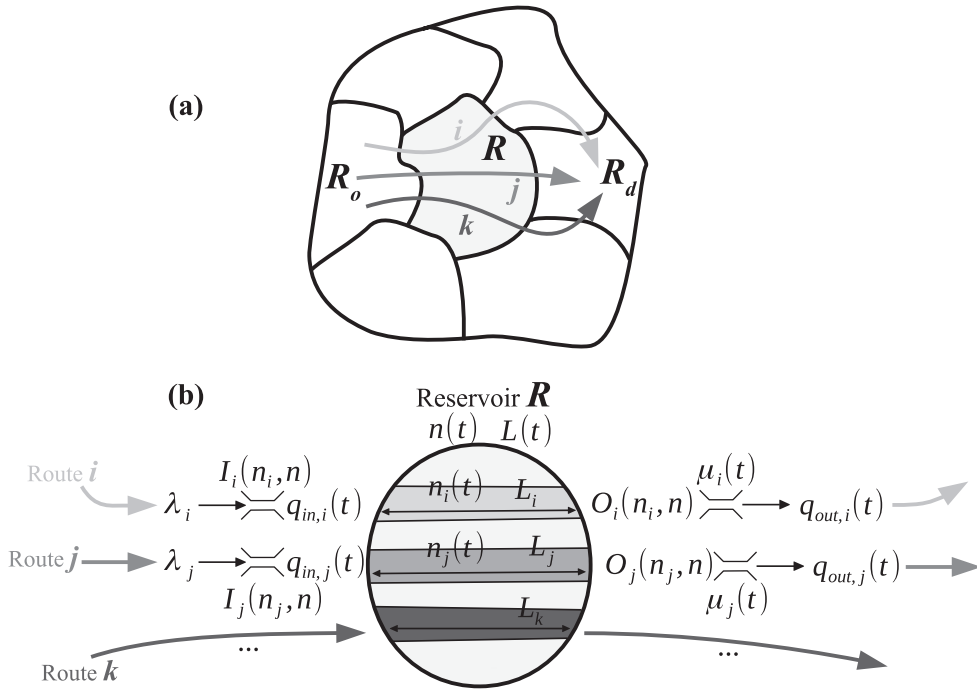


Fig. 5. (a) Examples of three routes (i, j, k) for a macroscopic OD (R_o, R_d) in a multi-reservoir system, (b) representation of the reservoir R crossed by the routes in the accumulation-based framework.

present study also applies for a reservoir with different accumulation categories (users are distinguished by their route or destination) but with a unique trip length (users are assumed to travel the same distance).

3.1.1. Traffic dynamics

Let us consider a single reservoir with N trip length categories L_i , or N routes with length L_i , as presented in Fig. 5(b). All accumulations n_i in each route i should satisfy the following system (Geroliminis, 2015):

$$\forall i \in \{1, \dots, N\}, \quad \frac{dn_i}{dt} = q_{in,i}(t) - q_{out,i}(t) \tag{11}$$

where $q_{in,i}(t)$ and $q_{out,i}(t)$ are respectively the effective inflow and outflow for route i . By definition we have: $n = \sum_{i=1}^N n_i$ (the total accumulation), $q_{in} = \sum_{i=1}^N q_{in,i}$ (the total effective inflow), and $q_{out} = \sum_{i=1}^N q_{out,i}$ (the total effective outflow). Depending on the route origin and destination (outside or inside the reservoir), its inflow and outflow treatment may be different. Therefore, to include any possible case, we define four sets of routes:

- \mathcal{P}_{in}^{ext} contains all the routes that originate outside the reservoir,
- \mathcal{P}_{out}^{ext} contains all the routes that end outside the reservoir,
- \mathcal{P}_{in}^{int} contains all the routes that originate inside the reservoir,
- \mathcal{P}_{out}^{int} contains all the routes that end inside the reservoir.

Any route i is included in two of the above-mentioned sets. For instance, transfer trips gather all the routes in \mathcal{P}_{in}^{ext} and \mathcal{P}_{out}^{ext} , while internal trips gather the routes in \mathcal{P}_{in}^{int} and \mathcal{P}_{out}^{int} (which is only one route in this case, because the sequence of reservoirs defining this route is reduced to one reservoir).

Conceptually, the reservoir is split into “sub-reservoirs” governed by the accumulation n_i . These sub-reservoirs are coupled together by the mean speed $V(n)$ or the total production $P(n)$. It is assumed that in slow-varying conditions, the trip completion rate G_i of each route i satisfies Little’s queuing formula (Geroliminis, 2015):

$$G_i(n_1, \dots, n_N) = G_i(n_i, n) = \frac{n_i}{L_i} V(n) = \frac{n_i}{n} \frac{P(n)}{L_i} \quad (\text{trip completion rate}) \tag{12}$$

Based on this formulation, a dynamic average trip length $L(t)$ can be defined by applying Little’s formula at the reservoir scale: $G(n) = n/L \cdot V(n)$. It comes (Geroliminis, 2009):

$$L(t) = \frac{n(t)}{\sum_{i=1}^N \frac{n_i(t)}{L_i}} = \frac{\sum_{i=1}^N G_i(n_i(t), n(t)) L_i}{G(n(t))} \quad (\text{average trip length}) \tag{13}$$

The aim of this section is the development of a congestion module that is robust and consistent with the underlying steady state assumption of this framework, transcribed in above Eqs. (12) and (13). The hypothesis of a quasi-static evolution of the system does not accommodate easily with the fast-varying transient phenomena that may appear during a congested event. One of the major changes compared to the framework in Section 2 is the difference in trip lengths. The conversion of production quantities such as the capacity P_c into flow units is no longer trivial, which is critical to define the entry supply function in this case.

3.1.2. Entry supply

As discussed in Section 2, the routes $i \in \mathcal{P}_{in}^{int}$ originating inside the reservoir should not have their inflow restricted if their demand $\lambda_i(t)$ is low enough and evolves slowly:

$$\forall i \in \mathcal{P}_{in}^{int}, \quad q_{in,i}(t) = \lambda_i(t) \tag{14}$$

We already explained this assumption in the previous section, but this needs to be further investigated in upcoming studies with simulation comparisons. In particular, the qualitative attributes of “low” and “slowly evolving” must be quantified, but this is out of the scope of the present work.

All the other routes $i \in \mathcal{P}_{in}^{ext}$ may experience an inflow limitation as they cross the entry border of the reservoir. However, unlike Section 2, a merging scheme must be used to allocate the available entry capacity to the routes coming from outside. The definition of a proper inflow merge has been poorly investigated in the literature. Previous studies usually consider a global supply function $I(n)$ at the reservoir entry that applies for all the routes entering the reservoir, and then split this supply using a demand pro-rata rule (Geroliminis, 2009; Knoop and Hoogendoorn, 2014; Yildirimoglu and Geroliminis, 2014; Ramezani et al., 2015). But nothing is said (i) on the shape of $I(n)$ and how it relates to the production-MFD $P(n)$ providing that there are different trip lengths inside the reservoir, and (ii) if another merging rule would be satisfying as well and why.

In this subsection, we look for the proper formulation of the individual supply limitation $I_i(n_1, \dots, n_N)$ applied to the entry of each route i . We first consider that all the routes cross the reservoir entry border for the beginning of our discussion. We have seen with some general test cases in Section 2.1.2 that the consistency between inflow and the reservoir internal dynamics is critical for the system stability in oversaturation. In the accumulation-based model, the internal dynamics are expressed through the steady state approximation with Little’s formula. This can be written either (i) at the route level with Eq. (12), or (ii) at the reservoir level through the dynamic average trip length $L(t)$ with Eq. (13). Assuming a given critical accumulation $n_{cs} > n_c$ as in the single trip length case, for (i) each individual limitation should be $I_i(n_i, n) = n_i/n \cdot P(n)/L_i$ for $n > n_{cs}$, and for (ii) the global limitation should be $\sum_{i=1}^N I_i(n_i, n) = P(n)/L$ for $n > n_{cs}$. Note that the first definition implies the second one, but that the reverse case is not true. Here, one can see that it is convenient to define the global entry supply function in production units to encompass both approaches. Let us then define the entry production supply $P_s(n)$ with a critical accumulation n_{cs} , and which shape can be designed like model 2 according to our discussion in Section 2.1.2. We notably have: $P_s(n) = P(n)$ for $n > n_{cs}$. But when applied to the routes in \mathcal{P}_{in}^{ext} only (that effectively cross the reservoir entry border), the entry production supply has to be modified accordingly to account for the internal origins: $P_s^{ext}(n) = P_s(n) - \sum_{i \in \mathcal{P}_{in}^{int}} L_i \lambda_i$. The accumulation ratio is modified into n_i/n^{ext} where $n^{ext} = \sum_{i \in \mathcal{P}_{in}^{ext}} n_i$. The second approach must also be rewritten for the routes in \mathcal{P}_{in}^{ext} only: $\sum_{i \in \mathcal{P}_{in}^{ext}} I_i(n_i, n) = P_s^{ext}(n)/L^{ext}$ for $n > n_{cs}$, where $L^{ext} = n^{ext} / \sum_{i \in \mathcal{P}_{in}^{ext}} \frac{n_i}{L_i}$. It follows that the two above-mentioned approaches for the expression of the consistency between inflow limitation and the internal dynamics lead to two possible definitions of the individual inflow supply:

$$\forall i \in \mathcal{P}_{in}^{ext}, \quad I_i(n_i, n) = \frac{n_i}{n^{ext}} \frac{P_s^{ext}(n)}{L_i} \quad (\text{endogenous entry supply}) \tag{15}$$

$$\forall i \in \mathcal{P}_{in}^{ext}, \quad I_i(n_i, n) = \alpha_i \frac{P_s^{ext}(n)}{L^{ext}} \quad (\text{exogenous entry supply}) \tag{16}$$

where the coefficients $\{\alpha_i\}_{i \in \mathcal{P}_{in}^{ext}}$ only verify $\sum_{i \in \mathcal{P}_{in}^{ext}} \alpha_i = 1$. These are called the merging coefficients α_i and may be independent of the reservoir state, so that the approach in Eq. (16) is called “exogenous”. As in the studies mentioned earlier, these coefficients can correspond to a demand pro-rata rule: $\forall i \in \mathcal{P}_{in}^{ext}, \alpha_i = \lambda_i / \sum_{j \in \mathcal{P}_{in}^{ext}} \lambda_j$, which is a common scheme in traffic flow theory (Jin and Zhang, 2003). In the following of the paper, the exogenous formulation will be always associated with a demand pro-rata rule. On the contrary, the approach in Eq. (15) is referred to as “endogenous” because its merging rule depends on the ratio of accumulations, that is, the inner state of the reservoir. When rewritten as $L_i I_i(n_i, n) = n_i/n \cdot P_s^{ext}(n)$, this approach conceptually corresponds to a merge in production, with the available production for route i being $L_i I_i(n_i, n)$ and the total available production $P_s^{ext}(n)$.

It is important to notice that the main difference between the exogenous and the endogenous formulations is the dimension (time or space) that is used to determine the share between the different routes. The endogenous model is grounded on Little’s formula and the steady state approximation inside the reservoir, which is the basic assumption for all the MFD theory. In steady state, the share between routes inside the reservoir and at the perimeter are equivalent and thus the ratios of accumulations n_i/n can be used to determine the fractions of entry flow at the perimeter. The exogenous model is more focused on the perimeter and does not impose the ratio in flows to be equivalent to the ratio in accumulations at all

times. The ratio in flows is then directly calculated based on the demand ratios. Thus, this model is more reactive to sudden changes in entry demand ratios. Based on our later analysis, this appears to be more suitable to get proper simulation results in a dynamic context.

3.1.3. Merging model and effective inflows

Once a model of entry supply $I_i(n_i, n)$ is chosen (endogenous or exogenous with a demand pro-rata), the effective inflow $q_{in,i}(t)$ of each route $i \in \mathcal{P}_{in}^{ext}$ could be simply calculated as the minimum between its demand $\lambda_i(t)$ and supply $I_i(n_i(t), n(t))$. While this method is appropriate when all these routes face a limitation at entry, it would be too restrictive when some of them are not limited. In the latter case, it would make sense to allocate more flow capacity to the congested routes (limited at entry) so that the total available capacity provided by the reservoir is fully used. This is a classical rule when merging inflows in traffic flow theory. Here, we thus propose to calculate the effective inflows with a given merge function $Merge(\cdot)$ that takes in arguments the demands, the merging coefficients and the available capacity. As detailed earlier, the expression of the endogenous supply functions implies a merge in entry productions, while the one of the exogenous supply functions a merge in inflows:

$$\{L_i q_{in,i}\}_{i \in \mathcal{P}_{in}^{ext}} = Merge\left(\{L_i \lambda_i\}_{i \in \mathcal{P}_{in}^{ext}}, \{n_i/n^{ext}\}_{i \in \mathcal{P}_{in}^{ext}}, P_s^{ext}(n)\right) \quad (\text{endogenous entry supply}) \quad (17)$$

$$\{q_{in,i}\}_{i \in \mathcal{P}_{in}^{ext}} = Merge\left(\{\lambda_i\}_{i \in \mathcal{P}_{in}^{ext}}, \{\alpha_i\}_{i \in \mathcal{P}_{in}^{ext}}, \frac{P_s^{ext}(n)}{L^{ext}}\right) \quad (\text{exogenous entry supply}) \quad (18)$$

For the function $Merge(\cdot)$, we use the merge algorithm presented in [Leclercq and Becarie \(2012\)](#) which consists of an extension of the fair merge of [Daganzo \(1995\)](#). For any set of M merging demands $\{\Lambda_i\}_{1 \leq i \leq M}$ with respective merge coefficients $\{\alpha_i\}_{1 \leq i \leq M}$ towards a unique entry with capacity C , the resulting effective inflows $\{Q_i\}_{1 \leq i \leq M}$ are calculated as:

$$\forall i \in \{1, \dots, M\}, \quad Q_i = \begin{cases} \Lambda_i & \text{if } \Lambda_i \leq \alpha_i C \\ \frac{\alpha_i}{\sum_{Q_j > \alpha_j C} \alpha_j} \left(C - \sum_{Q_j \leq \alpha_j C} Q_j \right) & \text{otherwise (fair merge)} \end{cases} \quad (19)$$

This merge algorithm ensures that the total available capacity C is always used when only certain inflows are limited while others are not. Its principle is that all demands Λ_i below their respective limitation $\alpha_i C$ are served, and then the remaining capacity is shared among the remaining inflows according to their merge coefficients. If some of these remaining inflows exceed their respective demand after sharing, then these demands are served and the remaining capacity is adjusted accordingly and shared among the remaining inflows. This process is repeated until all the inflows are served and/or the capacity C is fully used. Note that this algorithm is applied similarly for both productions and flows.

This single reservoir framework also includes a point-queue model for each route to store queuing vehicles at entry when the corresponding demand is not satisfied. Once a queue has formed for a specific route i , its demand λ_i is set to maximum, equal to the reservoir physical inflow capacity (sum of all entry link capacities), provided that the queue is not empty.

3.1.4. Exit demand, diverging model and effective outflows

The question of outflow diverging concerns all the routes within the reservoir, since it is the result of its internal dynamics. However, the difference between the two sets \mathcal{P}_{out}^{ext} and \mathcal{P}_{out}^{int} is that each route i ending outside the reservoir may undergo an exogenous outflow limitation $\mu_i(t)$ when crossing the exit boundary (representing inflow restriction to the next reservoir), while in general, the outflow of each route ending inside the reservoir is not exogenously limited:

$$\forall i \in \mathcal{P}_{out}^{int}, \quad \mu_i(t) = +\infty \quad (20)$$

Nevertheless, note that finite supply values μ_i for $i \in \mathcal{P}_{out}^{int}$ could be eventually used to simulate saturated parking inside the reservoir.

When considering the routes in \mathcal{P}_{out}^{ext} , the exit demand is the rate at which users want to cross the reservoir exit boundary to reach a neighboring reservoir. The exit demand is not measurable in practice, but it is an essential concept to define the reservoir outflow in oversaturation. While rarely mentioned in other works, it is implicitly involved as soon as the potential outflow of a reservoir may be limited by the entry capacity of a neighboring reservoir, as in the studies mentioned earlier (e.g., [Knoop and Hoogendoorn, 2014](#); [Yildirimoglu and Geroliminis, 2014](#); [Ramezani et al., 2015](#); [Sirmatel and Geroliminis, 2017](#)). In these studies, the outflow demand is considered equal to the trip completion rate $G_i(n_i, n)$. We thus refer to this approach as the “decreasing exit demand” (in oversaturation) for the outflow model. In this framework the effective outflows can be calculated as:

$$\begin{cases} \forall i \in \mathcal{P}_{out}^{ext}, & q_{out,i}(t) = \min[\mu_i(t); G_i(n_i(t), n(t))] \\ \forall i \in \mathcal{P}_{out}^{int}, & q_{out,i}(t) = G_i(n_i(t), n(t)) \end{cases} \quad (\text{for a decreasing exit demand}) \quad (21)$$

However, we pinpointed in [Section 2.1.3](#) a drawback of this formulation for the routes crossing the exit boundary. During the offset of a congestion peak, we showed with simple simulation scenarios that oversaturation in the reservoir results in

very low demand for outflow, and thus prevents it from a proper recovery after the peak. As in Eq. (5), we propose that the exit demand should be maximum in oversaturation for the routes in \mathcal{P}_{out}^{ext} :

$$\forall i \in \mathcal{P}_{out}^{ext}, \quad O_i(n_i, n) = \begin{cases} \frac{n_i}{n} \frac{P(n)}{L_i} = G_i(n_i, n) & \text{if } n < n_c \\ \frac{n_i}{n} \frac{P_c}{L_i} & \text{otherwise} \end{cases} \quad (\text{maximum exit demand}) \quad (22)$$

This new outflow model is therefore named the “maximum exit demand”. But unlike the decreasing exit demand model, here the calculation of the effective outflows is not straightforward. In oversaturation, our new formulation introduces too many degrees of freedom in the description of each route outflow. Actually, because users traveling on different routes in the same reservoir share the same mean speed, their respective rates at which they can exit the reservoir are not independent. We must have in steady state: $\forall i \in \{1, \dots, N\}, q_{out,i} = G_i(n_i, n) = n_i/L_i \cdot V(n)$, thus the inter-dependency relationships are as follows: $\forall i, j \in \{1, \dots, N\}, q_{out,i}/q_{out,j} = n_i/n_j \cdot L_j/L_i$. When some routes $i \in \mathcal{P}_{out}^{ext}$ are limited by μ_i , these relationships are verified in the decreasing exit demand model thanks to Eq. (21), where each exit is driven either by its limitation or by the trip completion rate. But in the maximum exit demand model, some routes may have an outflow disconnected from the mean speed evolution because of the maximum we set. When driven by the exit limitations, we could have $q_{out,i} = \mu_i$ and $q_{out,j} = \mu_j$ for some $i, j \in \mathcal{P}_{out}^{ext}$, but the ratio of two exogenous limitations μ_i/μ_j has a few chances to equal $n_i/n_j \cdot L_j/L_i$ in practice. Hence, we explicitly add the inter-dependency relationships to calculate the effective outflows with the maximum exit demand model:

$$q_{out,k}(t) = \min[\mu_k(t); O_k(n_k, n)] \quad (\text{most constrained outflow}) \quad (23)$$

$$\text{where: } k = \arg \min_{1 \leq i \leq N} \frac{\mu_i}{O_i(n_i, n)}$$

$$\forall i \in \{1, \dots, N\}, i \neq k, \quad q_{out,i}(t) = \frac{n_i(t)}{n_k(t)} \frac{L_k}{L_i} q_{out,k}(t) \quad (\text{for a maximum exit demand}) \quad (24)$$

This formulation is designed to ensure that none of the partial outflows $q_{out,i}(t)$ exceeds its corresponding exogenous limitation $\mu_i(t)$. To this end, it is based on the definition of the most constrained outflow. In congestion, the system will adapt to the limitation $\mu_k(t)$ for route k , so that at equilibrium we have $G_k(n_k, n) = n_k(t)/L_k V(n(t)) = \mu_k(t)$ (assuming that $\mu_k(t)$ is constant after a given time). Knowing that outflow k is chosen as the most constrained one, i.e. with the highest difference between demand $O_k(n_k, n)$ and supply μ_k (demand being higher than supply, see Eq. (23)), we have then: $\forall i \neq k, O_i/O_k = n_i/n_k \cdot L_k/L_i = q_{out,i}/q_{out,k} \leq \mu_i/\mu_k$, and thus $q_{out,i} \leq \mu_i$ because $q_{out,k} = \mu_k$. It results that all effective outflows i in Eq. (24) will be automatically lower than their respective limitations $\mu_i(t)$. However, while protecting the downstream reservoirs from an excess of flow and thus from a possible gridlock, the consequence of this approach is that the flow in many routes may be actually lower than their respective limitations. This is also observed when using Eq. (21) with the decreasing exit demand model. All this is illustrated in the upcoming Section 4.

Interestingly, we can show that the instantaneous application of the relationships in Eq. (24) is equivalent to the following identity at the reservoir scale:

$$\sum_{i=1}^N L_i q_{out,i}(t) = L(t) q_{out}(t) \quad (\text{total exit production}) \quad (25)$$

The latter implies that the expression of the dynamic average trip length $L(t)$ is always valid to define the total exit production.

3.2. Implementation in the trip-based model

The inflow and outflow models we have designed for the accumulation-based model are straightforward to implement in the trip-based model by using the “switching” method we presented in Sections 2.2 and 2.3. This is exactly what we propose to manage inflows considering the entry supply functions described by Eqs. (15) and (16). Outflow management can also be done by using a similar method and transforming demand flows into demand exit times that are matched with the supply times at exit. However, we want to promote here a different method, which is more in accordance with the trip-based framework and spirit. Basically, the idea is to ensure a First-In-First-Out (FIFO) discipline in vehicle arrival times. This does not mean that traffic conditions are FIFO in the reservoir, because of the different trip lengths. But this means that as the speed is uniform at each step of the simulation, the order of vehicles at the exit boundaries defined by remaining travel distances should be preserved. In practice, we maintain a global waiting list and a waiting list of vehicles per route. When a new vehicle enters the reservoir, the arrival times of the traveling vehicles are still unknown, but because the vehicles are all traveling at the same speed, they can be simply ordered by their remaining travel distance. Keeping the vehicle global order corresponds to the natural dynamics of the trip-based model, as in this framework the outflow is precisely defined by the rate at which vehicles complete their trip length. This global order can be seen as the equivalent of the accumulation ratios n_i/n that we find in the accumulation-based formulation through Little’s formula. In slow-varying conditions, both models lead to similar results as the underlying steady state conditions of Little’s formula holds (see Mariotte et al., 2017). This means that the sequence of routes in the global waiting list is in accordance with the accumulation ratios. In fast-varying

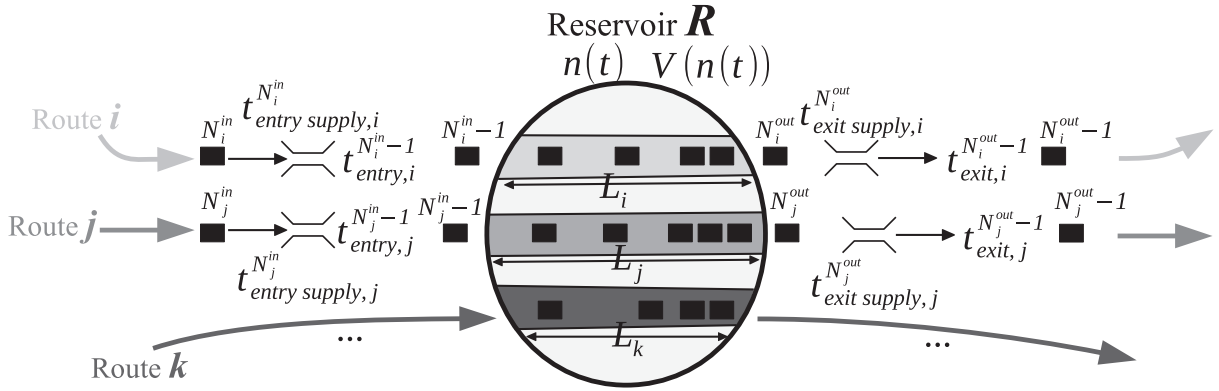


Fig. 6. Representation of the reservoir R crossed by the routes (i, j, k) in the trip-based framework.

conditions however, we expect different results because the accumulation ratios n_i/n can be instantaneously modified at both the entry and exit in the accumulation-based model, whereas it takes time to get a new order of routes (represented by traveling vehicles) in the waiting list of the trip-based model.

To illustrate this, let us consider a simple example of a reservoir crossed by two routes denoted 1 and 2. Suppose that we have $n_1/n = 0.75$ and $n_2/n = 0.25$ in the accumulation-based model when the system evolves slowly. Then, we would observe the following sequence of routes for the traveling vehicles in the trip-based model: [11121112...]. When some capacity restrictions appear at one exit, the modification of the accumulation ratios can evolve accordingly in the accumulation-based model, supposedly towards $n_1/n = n_2/n = 0.5$ in our example. Thus the limitation that we apply at entry is consistent with what is happening at exit, i.e. a flow of the kind $n_i/n \cdot V(n)$. But while we apply the same limitation at entry in the trip-based model, the situation at exit is still given by the previous order [11121112...], and we have to wait for these vehicles to exit before the new selection at entry provides the new expected order [12121212...]. This delay between entry and exit is one of the fundamental differences between both modeling approaches. This is the reason we prefer the outflow model preserving the exit vehicle order in the trip-based framework, which is explicitly designed to account for such delays.

3.2.1. Effective entry times

At the reservoir entry, in the event-based scheme of the trip-based model, the $\{N_i^{in}\}_{1 \leq i \leq N}$ represent the numbers of the next vehicles to enter each route i . Their corresponding entry demand times are calculated as: $t_{entry\ dem,i}^{N_i^{in}} = t_{entry,i}^{N_i^{in}-1} + 1/\lambda_i(t)$, where $t_{entry,i}^{N_i^{in}-1}$ is the effective entry time of the previous vehicle in route i . As regards the inflow merging scheme, recall that we designed two entry flow functions for the accumulation-based model. The first one, called the endogenous supply formulation, provides a supply value per entry and can be implemented in the trip-based model as follows. Each route i may restrain its inflow by a supply time $t_{entry\ supply,i}^{N_i^{in}}$ for the N_i^{in} th vehicle willing to enter. This supply time is calculated with the entry supply $I_i(n_i, n)$ presented in Eq. (15):

$$\forall i \in \mathcal{P}_{in}^{ext}, \quad t_{entry\ supply,i}^{N_i^{in}} = t_{entry,i}^{N_i^{in}-1} + \frac{1}{I_i(n_i, n)} \quad (\text{entry supply time}) \tag{26}$$

where $t_{entry,i}^{N_i^{in}-1}$ is the entry time of the previous vehicle in route i , see also Fig. 6. In case only some of the routes are congested, we can also apply the fair merge as described in Section 3.1.3 to ensure that the total entering production capacity is used. In practice, this is achieved in the event-based resolution scheme by modifying the entry supply times of the congested routes. This modification is done directly in the entry supply function $I_i(n_i, n)$ used in Eq. (26):

$$\forall i \in \mathcal{P}_{in}^{ext}, \quad I_i(n_i, n) = \begin{cases} \lambda_i & \text{if } \lambda_i \leq I_i(n_i, n) \\ \frac{n_i}{\sum_{q_{in,j} > I_j(n_j, n)} n_j} \frac{1}{L_i} \left(p_s^{ext}(n) - \sum_{q_{in,j} \leq I_j(n_j, n)} L_j q_{in,j} \right) & \text{otherwise} \end{cases} \tag{27}$$

where $p_s^{ext}(n)$ is the modified entry production supply introduced in Section 3.1.2. Then, the next reservoir entry time is the minimum of the possible entry times of all the routes:

$$t_{entry,k}^{N_k^{in}} = \min_{1 \leq i \leq N} \left[\max \left[t_{entry\ dem,i}^{N_i^{in}}, t_{entry\ supply,i}^{N_i^{in}} \right] \right] \quad (\text{for an endogenous entry supply}) \tag{28}$$

The second entry supply formulation, referred to as exogenous, is based on a global supply value at entry split among the routes with exogenous merging coefficients. As in the accumulation-based model, the merging coefficients are defined

with a demand pro-rata rule. This formulation can be implemented in the trip-based model as follows. A unique entry supply is applied to all the routes, calculated as $P_s^{\text{ext}}(n)/L^{\text{ext}}$, see Eq. (16). The supply time $t_{\text{entry supply}}$ for the next entry in the reservoir is thus:

$$t_{\text{entry supply}} = t_{\text{last entry}} + \frac{L^{\text{ext}}}{P_s^{\text{ext}}(n)} \quad (\text{global entry supply time}) \quad (29)$$

where $t_{\text{last entry}}$ is the last effective entry time in the reservoir. The translation of the demand pro-rata rule in the trip-based model consists in allowing the vehicles entering the reservoir according to their demand entry times. Then the next reservoir entry time is the minimum of the demand times, eventually modified by the global supply time:

$$t_{\text{entry},k}^{N_k^{\text{in}}} = \max \left[t_{\text{entry dem},k}^{N_k^{\text{in}}}; t_{\text{entry supply}} \right] \quad (\text{for an exogenous entry supply}) \quad (30)$$

$$\text{where: } k = \arg \min_{1 \leq i \leq N} t_{\text{entry dem},i}^{N_i^{\text{in}}}$$

3.2.2. Effective exit times

At the reservoir exit, the vehicles are kept in order inside the reservoir until the next exit is possible. As regards the outflow diverging scheme, recall that we presented two formulations in the accumulation-based model, namely based on a decreasing exit demand model in Eq. (21), and based on a maximum exit demand model in Eq. (24). In the trip-based approach, the two exit demand models can be distinguished with the definition of the first vehicle N_k^{out} to exit the reservoir (traveling on a given route k). Here, the $\{N_i^{\text{out}}\}_{1 \leq i \leq N}$ represent the numbers of the next vehicles to exit in each route i . Their corresponding exit supply times are calculated as: $t_{\text{exit supply},i}^{N_i^{\text{out}}} = t_{\text{exit},i}^{N_i^{\text{out}-1}} + 1/\mu_i(t)$, where $t_{\text{exit},i}^{N_i^{\text{out}-1}}$ is the effective exit time of the previous vehicle in route i and $\mu_i(t) = +\infty$ if $i \in \mathcal{P}_{\text{out}}^{\text{int}}$. see also Fig. 6.

In the decreasing exit demand model, the exit demand time $t_{\text{exit dem},i}^{N_i^{\text{out}}}$ of each route i is calculated with the current mean speed value $V(n)$ and the remaining distance that the first vehicle of each waiting list has to travel:

$$\forall i \in \{1, \dots, N\}, \quad t_{\text{exit dem},i}^{N_i^{\text{out}}} = t + (L_i - L^{N_i^{\text{out}}})/V(n) \quad (\text{for a decreasing exit demand}) \quad (31)$$

where t is the current time and $L^{N_i^{\text{out}}}$ is the remaining distance to travel for vehicle N_i^{out} . Then, the next reservoir exit time is the minimum of the possible exit times of all the routes:

$$t_{\text{exit},k}^{N_k^{\text{out}}} = \min_{1 \leq i \leq N} \left[\max \left[t_{\text{exit dem},i}^{N_i^{\text{out}}}; t_{\text{exit supply},i}^{N_i^{\text{out}}} \right] \right] \quad (\text{for a decreasing exit demand}) \quad (32)$$

In the maximum exit demand model, the exit demand time $t_{\text{exit dem},i}^{N_i^{\text{out}}}$ of each route i is calculated with the same Eq. (31), excepting that the vehicles traveling on the routes $i \in \mathcal{P}_{\text{out}}^{\text{ext}}$ are pushed to their destinations if $n > n_c$, with a maximum exit rate fixed at $n_i/n_c \cdot P_c/L_i$ as in the accumulation-based model, see Eq. (22). This reproduces the maximum outflow demand in oversaturation as explained in Section 2.3. It follows:

$$\begin{cases} \forall i \in \mathcal{P}_{\text{out}}^{\text{ext}}, & t_{\text{exit dem},i}^{N_i^{\text{out}}} = \max \left[t; t_{\text{exit},i}^{N_i^{\text{out}-1}} + \frac{n}{n_i} \frac{L_i}{P_c} \right] \\ \forall i \in \mathcal{P}_{\text{out}}^{\text{int}}, & t_{\text{exit dem},i}^{N_i^{\text{out}}} = t + (L_i - L^{N_i^{\text{out}}})/V(n) \end{cases} \quad (\text{for a maximum exit demand}) \quad (33)$$

Then, the next reservoir exit time is defined as the most constrained one, just as in the accumulation-based formulation of the maximum demand exit model:

$$t_{\text{exit},k}^{N_k^{\text{out}}} = \max \left[t_{\text{exit dem},k}^{N_k^{\text{out}}}; t_{\text{exit supply},k}^{N_k^{\text{out}}} \right] \quad (\text{for a maximum exit demand}) \quad (34)$$

$$\text{where: } k = \arg \min_{1 \leq i \leq N} t_{\text{exit dem},i}^{N_i^{\text{out}}}$$

4. Simulation results with for a two-route system

The different modeling approaches for inflow merging and outflow diverging we presented above are now illustrated on a simple simulation case with two routes. The MFD characteristics are the same as in Section 2.3: $n_j = 1000$ veh, $n_c = 400$ veh, $P_c = 3000$ veh.m/s and $u = 15$ m/s. The shape of the entry supply function $P_s(n)$ is similar to model 2 presented in Section 2.1.2. Two routes corresponding to transfer trips are considered as shown in Fig. 7(a). Route 1 has a length of $L_1 = 2000$ m, and route 2 of $L_2 = 1000$ m. Two scenarios are investigated, a demand surge with constant supply limitation at exit first, and a demand surge followed by a temporary supply reduction at exit then. For each scenario, three reservoir models are compared as detailed below:

- Model 1/1: uses exogenous (demand pro-rata) merging at entry, and decreasing exit demand at exit.
- Model 1/2: uses exogenous (demand pro-rata) merging at entry, and maximum exit demand at exit.
- Model 2/2: uses endogenous merging at entry, and maximum exit demand at exit.

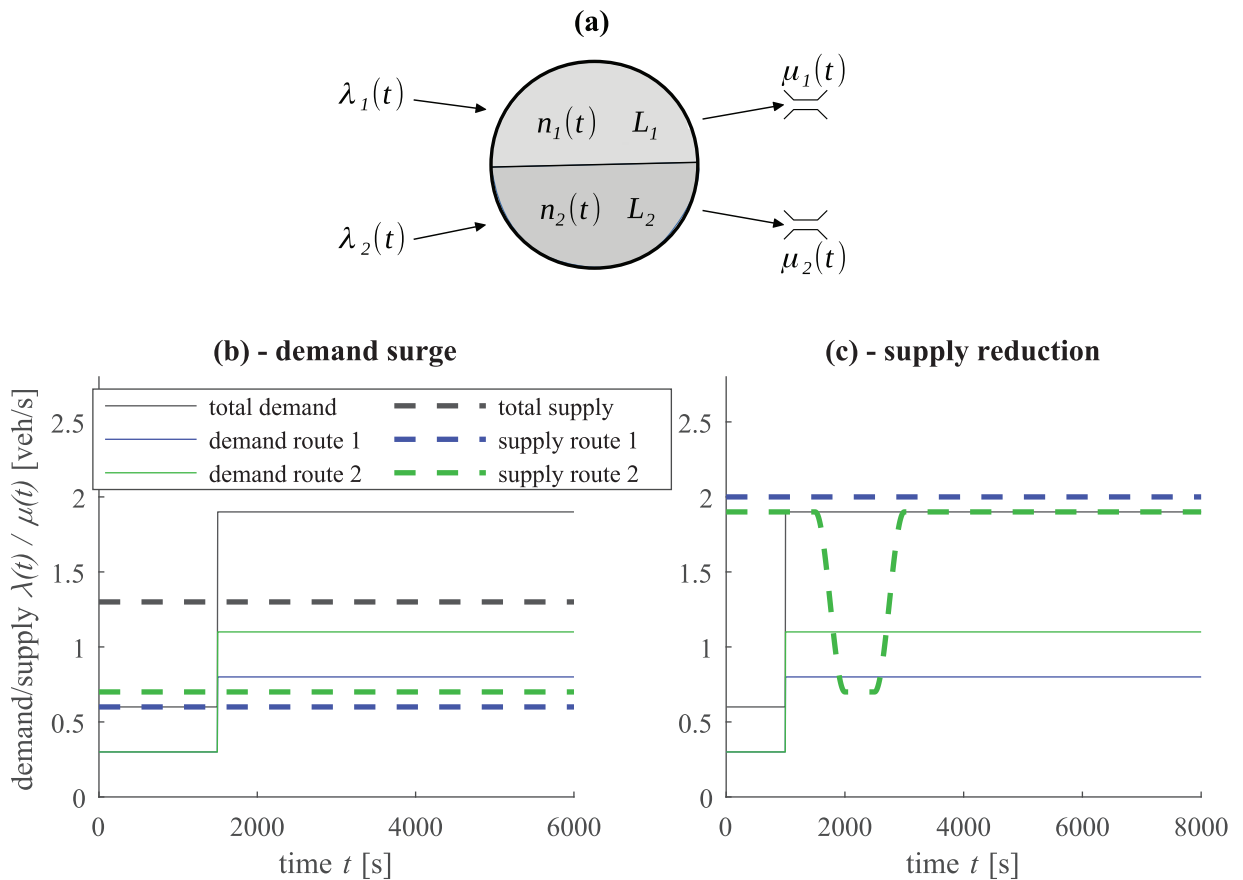


Fig. 7. (a) Two routes in a reservoir. (b) Case of a demand surge with constant supply limitation, and (c) a demand surge followed by a supply reduction with demand $\lambda_i(t)$ and supply $\mu_i(t)$ profiles.

4.1. Case of a demand surge with constant supply limitation

Fig. 7(b) presents a scenario of a demand surge on both routes. After 1500 s we have $\lambda_1(t) = 0.8$ veh/s and $\lambda_2(t) = 1.1$ veh/s, whereas the exit supplies are $\mu_1(t) = 0.6$ veh/s and $\mu_2(t) = 0.7$ veh/s. Note that such extreme and rather unrealistic boundary settings will bring the reservoir state close to gridlock, nevertheless this numerical application is only intended to illustrate the behavior of inflow merging and outflow diverging in oversaturation. The simulation results are given in Fig. 8(a)-(c) for the reservoir model 1/1, in Fig. 8(d)-(f) for model 1/2, and in Fig. 8(g)-(i) for model 2/2. Each model is run with the accumulation-based and trip-based approaches. All the three models reach a consistent steady oversaturated state at the end of the simulation, in the sense that the flow on each route i satisfies: $q_{in,i} = q_{out,i} = n_i/L_i \cdot V(n)$. Interestingly, we note that even though the boundary conditions are the same in all cases, different equilibriums are found depending on the entry merging or exit diverging schemes, and the accumulation-based or trip-based approaches as well. This non-uniqueness of the equilibrium in oversaturation is discussed in more details with a simple example in Appendix A.

Regarding inflow merging at entry, the choice of the demand pro-rata or the endogenous formulation has a clear impact on the results. Before $t = 2000$ s, the inflow on each route equals its respective demand. Then starting from shortly after 2000 s, the entry supply function reduces the inflows to adapt to the outflow limitations. On the whole, it can be seen with models 1/1 and 1/2 that the demand pro-rata formulation leads to an equal allocation of the supply to both routes, see Fig. 8(b) and (e). This is due to the point queue models at the entry to each route: when the inflows start being limited, the demands become both equal to the same maximum, where by default this maximum corresponds to $P_s(n)$ divided by the current value of $L(t)$. Actually, the two queues do not form exactly at the same time, and thus the demands do not become equal at the same time: there is a short transition period after 2000 s where oscillations in inflows are observed. These oscillations are the result of the instantaneous application of the demand pro-rata rule in the accumulation-based model, as the demands alternate between the maximum and their original values when the queues are filling in and emptying during this transition period. As route 2 is shorter than route 1, the consequence of an equal distribution $q_{in,1} = q_{in,2}$ is that less users travel on route 2 compared to route 1, i.e. $n_2 < n_1$ at equilibrium. On the contrary, the endogenous formulation in model 2/2 shows a different allocation between routes 1 and 2, see Fig. 8(h). This leads to similar accumulations in steady

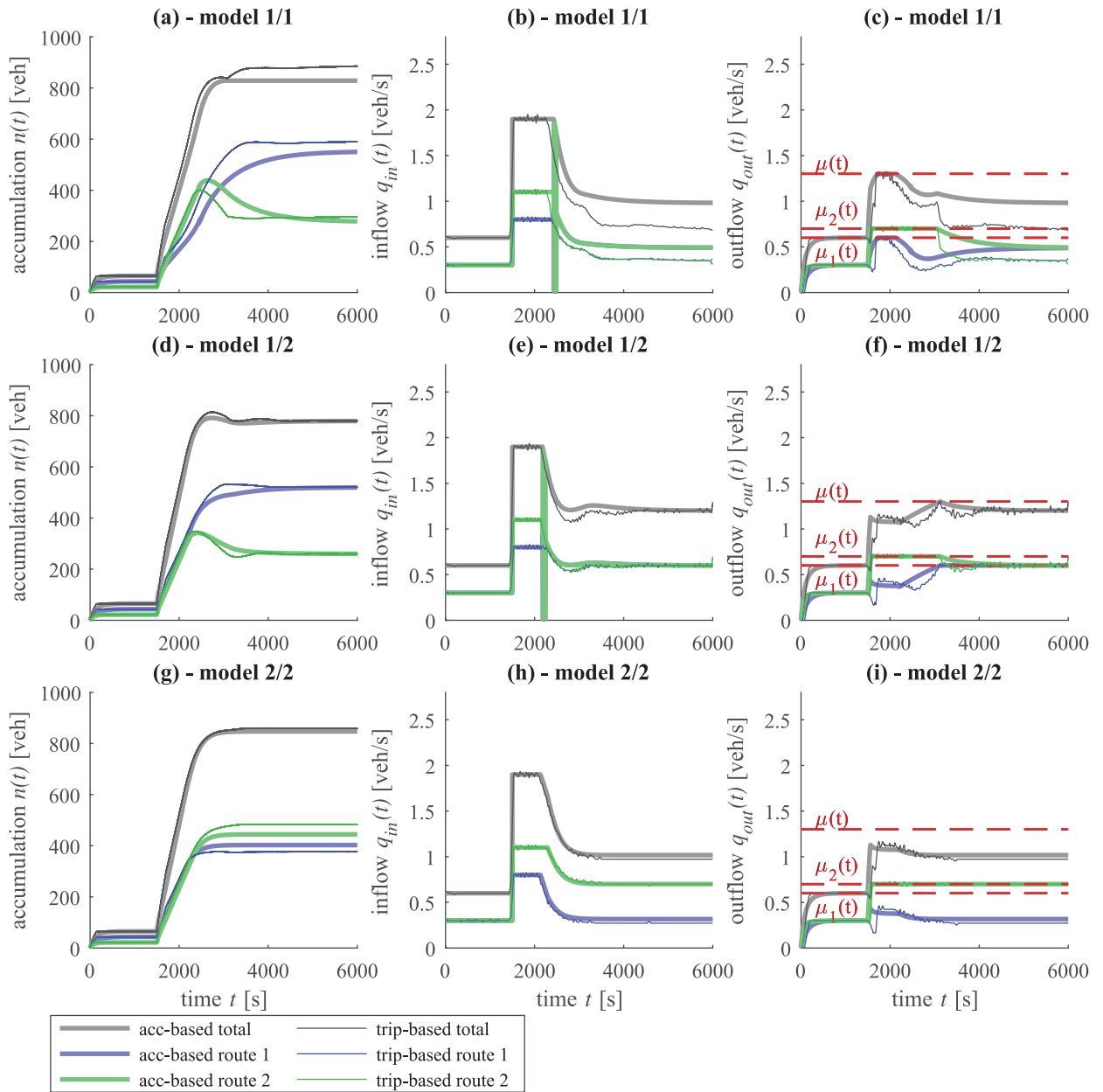


Fig. 8. Case of demand surge with constant supply limitation at exit. (a) Evolution of accumulation, (b) inflow and (c) outflow for model 1/1; (d) Evolution of accumulation, (e) inflow and (f) outflow for model 1/2; (g) Evolution of accumulation, (h) inflow and (i) outflow for model 2/2.

state. Here the point queue models have no influence on the flow allocation, which is independent from the demands by definition of the endogenous formulation.

Focusing on outflow diverging at exit then, the choice of the decreasing or maximum exit demand model also has a noticeable impact on the results, especially during the transient phase around 2000 s. Right after the demand surge at 1500 s, the outflows of both routes increase as well but become rapidly limited by the exogenous constraints μ_1 and μ_2 . Note that the rise of outflows is instantaneous in the accumulation-based model, whereas a delay is visible before the outflows increase in the trip-based model. This difference in the dynamics between both approaches was extensively studied in [Mariotte et al. \(2017\)](#). With the decreasing exit demand formulation in model 1/1, we see that both outflows $q_{out,1}(t)$ and $q_{out,2}(t)$ can reach their respective limitations $\mu_1(t)$ and $\mu_2(t)$, see [Fig. 8\(c\)](#). However as mentioned earlier in [Section 3.1.4](#), unless the ratio $\mu_1(t)/\mu_2(t)$ equals $n_1(t)/n_2(t) \cdot L_2/L_1$, this situation has a few chances to be a consistent equilibrium for the reservoir. Actually, we observe a transition period from 2000 s to 5000 s where the mean speed adapts to the exit limitations, and as a result makes the outflows decrease. Then the system ends in a kind of “sub-optimal” state, because each

route steady outflow is found below its limitation. On the other hand, the maximum exit demand formulation in models 1/2 and 2/2 ensures that at least one of the outflows reaches its limitation. This route exit is denoted as the most constrained one, and determined with Eq. (23). In Fig. 8(i) with model 2/2, the most constrained outflow is $q_{out,2}$. In Fig. 8(f) with model 1/2, this one is $q_{out,2}$ until 3000 s where it finally becomes $q_{out,1}$ because of the different dynamics due to the different inflow merging. However, the counterpart of the maximum exit demand formulation is that the inter-dependency relationships in Eq. (24) are instantaneously applied to the other outflows. Thus unlike model 1/1, no transient period is observed during which each route outflow $q_{out,i}(t)$ equals its limitation $\mu_i(t)$, because the inter-dependency relationships in models 1/2 and 2/2 bring the system in a quasi-steady state. This illustrates one of the major differences between the two outflow diverging schemes: the decreasing exit demand model is flexible enough to reproduce the dynamics of transient states but too constrained to reproduce the reservoir discharge after oversaturation. On the other hand, the maximum exit demand model allows higher outflows to mimic users queuing to exit the reservoir, but happens to be too restrictive to reproduce highly dynamic transient states.

On the whole, the accumulation-based and trip-based approaches provide quite similar results for a given inflow and outflow model. Nevertheless, it must be noticed that the final states are not exactly the same in both models. This is particularly visible for model 1/1, see Fig. 8(a)–(c). This is due to the trip-based dynamics where, unlike the accumulation-based approach, a delay between the reservoir entry and exit is responsible for a different transient state evolution, see also our discussion at the beginning of Section 3.2. As mentioned earlier, the equilibrium of the multi-route system in oversaturation is not unique with the same boundary conditions and notably depends on what happens during the transient phase. The difference of behavior during this phase between the accumulation-based and trip-based models explains that they reach different steady states.

4.2. Case of a demand surge followed by a temporary supply reduction

The second scenario used to illustrate the differences between the modeling approaches consists of a temporary supply reduction at exit, as presented in Fig. 7(c). The demand settings are the same as in the previous scenario. The supply limitations are all removed in this case, except from a temporary flow reduction happening on route 2 around 2000 s. The evolutions of accumulation, inflow and outflow in both accumulation-based and trip-based frameworks are given in Fig. 9(a)–(c) for the reservoir model 1/1, in Fig. 9(d)–(f) for model 1/2, and in Fig. 9(g)–(i) for model 2/2. All the different approaches provide quite similar results up to 2000 s when the limitation applies. But then, two different evolutions are clearly distinguished, depending on the choice of the outflow model. The system is able to recover once the limitation ends after 3000 s with the maximum exit demand approach in models 1/2 and 2/2, while the situation is stuck to an oversaturated state with the decreasing exit demand approach in model 1/1. In Fig. 9(f) and (i), we actually observe an increase of outflow after the limitation on route 2 is released, which is due to the high demand to exit the reservoir for the vehicles on route 2. However, the outflow remains too low in model 1/1, thus preventing the queues inside the reservoir from exiting, see Fig. 9(c). Like the example in Section 2.3, this scenario highlights the advantage of our new outflow model compared to the conventional approach from the literature.

Apart from the oscillations in inflow also noticed in the previous scenario, the differences between the two inflow merging schemes in models 1/2 and 2/2 are less visible in this case. The action of the inflow limitation is noticeable during the onset of congestion between 2000 s and 3000 s, but then the evolution of the system is mainly driven by the outflow diverging scheme. Besides, the differences between the accumulation-based and trip-based approaches are more obvious in this scenario because of a longer transient period. The difference of dynamics between the routes and the effect of the order of vehicles in the trip-based model lead to a longer recovery phase in this model compared to the accumulation-based one.

5. Comparisons with existing models

In this section, we present an application of our framework in a simple multi-reservoir environment. We aim at illustrating some phenomena we observed with the previous two-route case, and also compare our framework with two other models from the literature.

5.1. Test case configuration and scenario

The reservoir system configuration is presented in Fig. 10(a). It basically consists of two macroscopic routes [$R_1 R_3 R_4 R_5 R_7$] (route 1) and [$R_2 R_3 R_4 R_6 R_8$] (route 2) that share some reservoirs in common. The idea is to see the influence of the modeling choices on the flow exiting from R_4 and its consequences on the two downstream reservoirs R_5 and R_6 . The characteristics of the reservoirs are mentioned in Table 1.

The demand scenario is presented in Fig. 10(b). This scenario together with the reservoir configurations are designed to create congestion on both routes due to the low entry capacity of R_7 and R_8 (equal to P_c , see Table 1). Thanks to these capacities and the high jam accumulation of R_3 , the origins R_1 and R_2 and destinations R_7 and R_8 are kept free of congestion during the whole simulation period. All queuing vehicles are then stored in R_3 , R_4 , R_5 and R_6 .

The two-route case from Section 4 is reproduced in R_4 with $L_1 = 1000$ m different from $L_2 = 600$ m. In the following, we will focus on the evolution of the total accumulation in reservoirs R_4 , R_5 and R_6 only. Many more things could be described

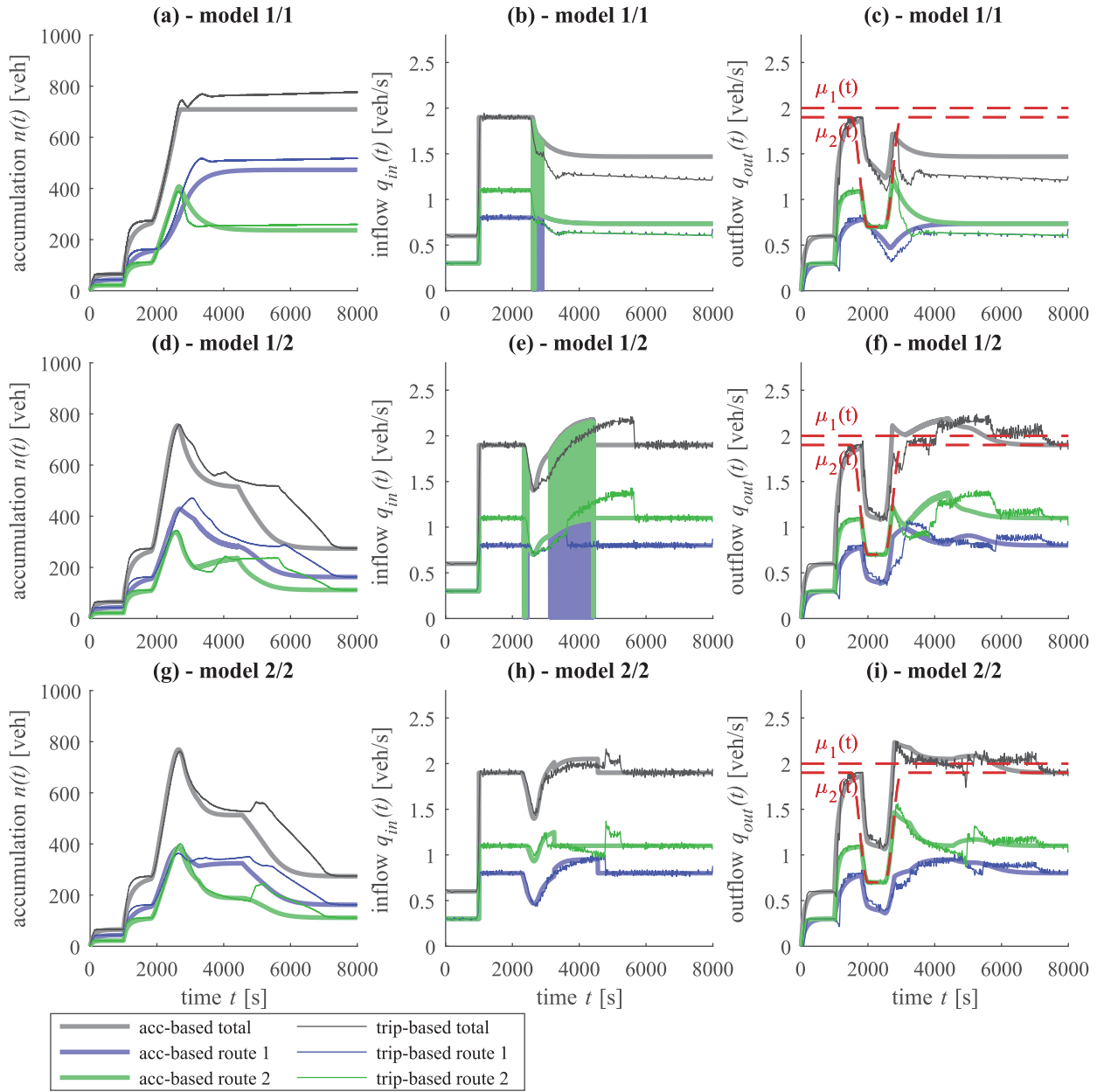


Fig. 9. Case of demand surge followed by a temporary supply reduction at exit. (a) Evolution of accumulation, (b) inflow and (c) outflow for model 1/1; (d) Evolution of accumulation, (e) inflow and (f) outflow for model 1/2; (g) Evolution of accumulation, (h) inflow and (i) outflow for model 2/2.

Table 1
Reservoir characteristics, where L_1 refers to route 1 and L_2 refers to route 2.

Characteristics	[units]	R_1	R_2	R_3	R_4	R_5	R_6	R_7	R_8
Jam accumulation n_j	[veh]	1000	1000	4000	1000	500	500	500	500
Max. production P_c	[veh.m/s]	3000	3000	3000	3000	3000	3000	600	600
Free-flow speed u	[m/s]	15	15	15	15	15	15	15	15
Trip length L_1	[m]	500	-	500	1000	500	-	1000	-
Trip length L_2	[m]	-	500	500	600	-	500	-	1000

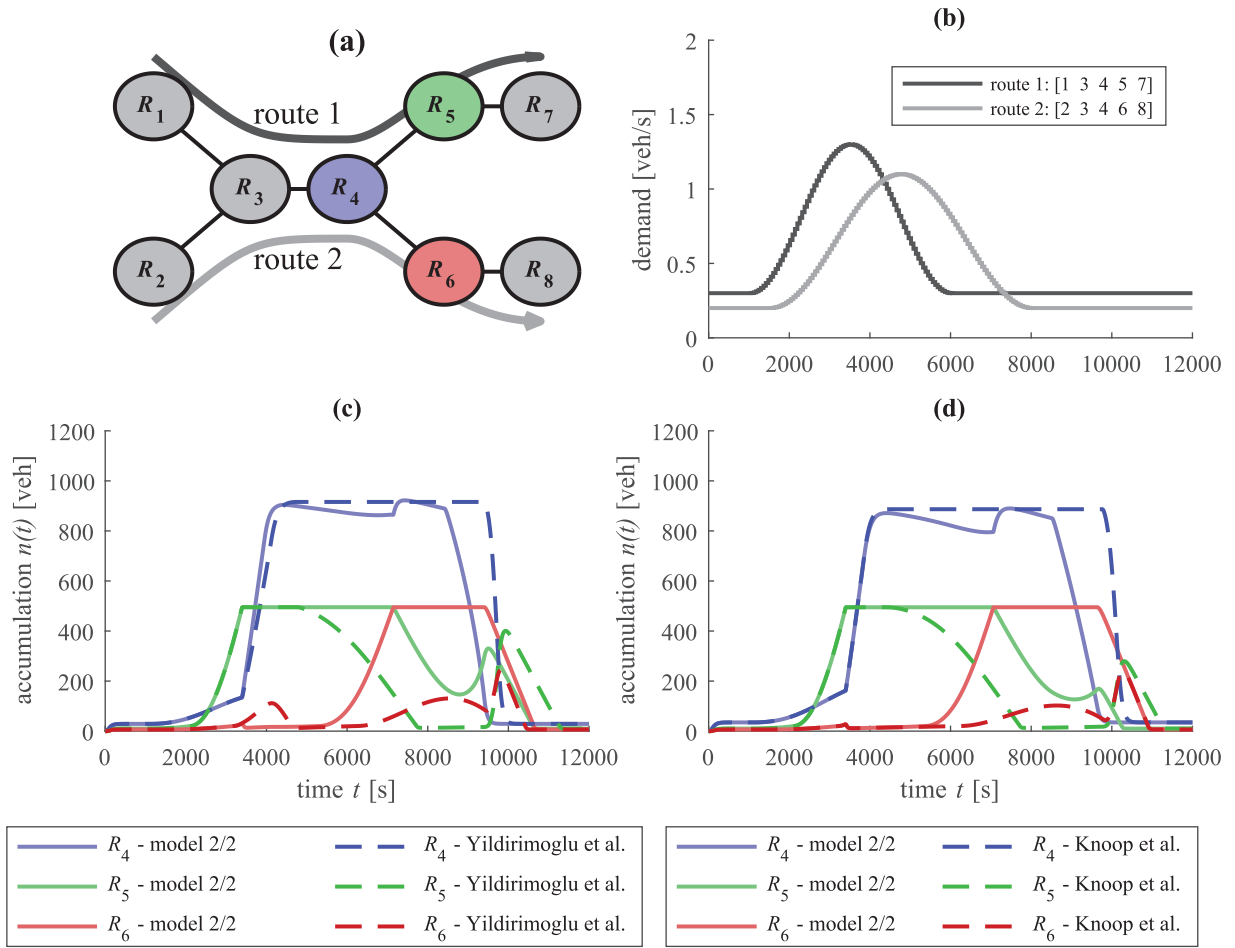


Fig. 10. (a) Reservoir system configuration, (b) demand profiles for the two routes. (c) Accumulation in reservoirs 4, 5 and 6, comparison between our model 2/2 and the model of Yildirimoglu and Geroliminis (2014), and (d) comparison between our model 2/2 and the model of Knoop and Hoogenboom (2014) with identical trip lengths in R_4 for both models.

in this system, but the idea is to keep the simulation analysis simple and exhibit some features of the two-route case that have already been explained in details in the previous section.

5.2. Comparison between model 2/2 and two other frameworks from the literature

We compare model 2/2, with the endogenous entry supply and the maximum exit demand, in the accumulation-based model with two simulators from the literature. The first one is developed in Yildirimoglu and Geroliminis (2014) and can account for different trip lengths within a reservoir. This framework is based on a demand pro-rata merge for inflows and a decreasing exit demand model for outflows, thus quite similar to model 1/1. The results are shown in Fig. 10(c). It clearly appears that our considerations about inflow and outflow definition have a significant impact on the simulation results, compared to what is usually done in the literature. To analyze these results, we choose to focus on the most important discrepancy between the two simulations: the congestion of R_6 which is predicted in our model but not in the other. This can be mainly explained by the different treatments of the flow entering into R_4 and exiting from R_4 . At $t = 3000$ s, the sharp increase of accumulation in R_5 is due to the limitation at the entry of R_7 . Because the flow transferring from R_4 to R_5 becomes limited too, congestion propagates into R_4 until a highly oversaturated steady state at $t = 4000$ s. Up to this time, our simulation and the other one experience quite the same evolution. However, during the propagation of congestion in R_4 the outflow from route 2 is not treated the same way in our model. Because of the instantaneous application of the inter-dependency relationships in R_4 as described by Eq. (24), this outflow has to adapt to the dynamics of R_4 (the sudden decrease of the mean speed), and is thus also reduced. Whereas in the model of Yildirimoglu and Geroliminis (2014), the effect of inter-dependency is not immediate, and the two outflows from R_4 can therefore behave independently, the outflow on route 1 being restricted, while the one on route 2 can remain a bit higher. It entails that the queue on route 2 in R_4 is growing faster in our model because of the lower outflow, which consequently allows more flow to enter (remember that

the entry supply is proportional to the ratio n_i/n , i.e. the more vehicles on route i , the more can enter). The situation is a bit different in the other model as the inflow share is operated through a pro-rata merge, but the smaller queue on route 2 in R_4 is also responsible for a lower inflow. In the end, once the exit to R_5 (route 1) is no longer the most constrained one after $t = 6000$ s, the queue on route 2 in R_4 can directly exit into R_6 , which creates congestion in R_6 due to the limitation at the entry of R_8 . Whereas in the other model, the flow into R_6 remains low, thus avoiding the creation of congestion. The counterpart is that the vehicles are stored in R_4 for a longer period, up to 11,000 s as shown by the evolution of accumulation (blue dashed line).

The second simulator is presented in Knoop and Hoogendoorn (2014) and can distinguish flows between simple routes but assumes the same trip length for all travelers in each reservoir. It is also based on a demand pro-rata rule for merging inflows and a decreasing exit demand model, therefore similar to model 1/1. In this second case, we make some minor modifications in the reservoir settings to ensure a fair comparison: we set $L_1 = L_2 = 1000$ m in R_4 . The results are shown in Fig. 10(d). The differences between both models look quite similar as in the previous comparison. But in this case, they are mainly explained by the inflow treatment at the entry of R_4 . Like in our previous analysis, our model allows more flow to enter R_4 on route 2, whereas the other one uses a pro-rata merge at the entry of R_4 which results in a different inflow share. Such a situation, as described above, creates a longer queue on route 2 in R_4 in our model, which is then responsible of the congestion appearing in R_6 .

The comparison examples in this last section illustrate the importance of the merging and diverging schemes in a multi-reservoir environment and show that some formulations can be disregarded by design as they lead to traffic dynamic patterns that are not realistic. In particular, we have shown that (i) other inflow merging schemes could be used and should not be ignored, and (ii) our new outflow model with a maximum exit demand is promising to reproduce a reliable behavior of queuing vehicles at the reservoir exit.

6. Conclusion

This study proposed a general framework to handle flow exchanges in multi-reservoir systems for the accumulation and trip-based models, in particular when congestion spills back. We focused on a single reservoir crossed by multiple commodities (e.g. macroscopic routes or trip categories with potentially different trip lengths) because it corresponds to the building block of any multi-reservoir simulator. This paper provides several contributions. At the reservoir entry first, different models of entry supply functions are proposed and discussed, together with two merging schemes consistent with the reservoir internal dynamics. At the reservoir exit then, a new model of outflow diverging is developed and compared to the conventional approach from the literature. This new model is intended to overcome the unrealistic oversaturation in which the reservoir can be trapped when some temporary supply reductions block the exit of transferring trips. Finally, the last contribution is the robust implementation of our new inflow merging and outflow diverging schemes, with the ones from the literature, in the trip-based framework. Even though this framework uses the same entry supply function as in the accumulation-based one, significant differences are expected during transient phases due to different representations of traffic dynamics in both frameworks, as discussed and shown with simulation examples.

This study constitutes a step forward a deeper understanding on flow exchanges in multi-reservoir systems with multiple regional routes. As illustrated with a simple multi-reservoir configuration at the end of the paper, significant differences in simulation results are expected depending on the choice made by the modeler. This study is focused on a theoretical analysis of MFD-based models and in particular on the entry and exit functions. We challenge the existing formulations against simple but meaningful test cases and highlight some limitations. We have then proposed some extensions to circumvent these issues and make sure that the multi-reservoir framework can work with both accumulation-based and trip-based MFD models. The next step is now to provide a complete validation of the different frameworks. As getting specific data to analyze flow exchanges at the reservoir borders is not an easy task, we are currently working on designing specific microsimulation test cases to challenge MFD formulations both at the reservoir entries and exits. The results will be presented in an upcoming paper.

Further developments of our MFD-based simulator will include a macroscopic route choice set generator and a DTA module for several applications like routing strategies, search-for-parking or perimeter control. The application of our framework with a control system can be envisioned in two different ways: the first one is the comparison of the control strategy when our approach is used instead of a simpler one; and the second one is the preliminary validation of different control strategies (based on a simple model) by simulating the resulting traffic states with a more detailed multi-reservoir and multi-route framework. Despite the relative complexity of the latter, this second option is considerably less demanding than setting a microscopic simulation in terms of computational effort and demand estimation.

Acknowledgements

The authors would like to warmly thank the two anonymous reviewers for their thorough comments, and especially the first reviewer who helped clarify the methodology by his/her careful reading. This significantly improved the overall quality and readability of the paper. This project has received funding from the European Research Council (ERC) under the European Union's Horizon 2020 research and innovation program (grant agreement No 646592 – MAGNUM project).

Appendix A. Illustration of outflow share

When using the maximum exit demand approach, it is interesting to note that it is almost impossible to identify in advance the most constrained exit, prior to the simulation. While this exit can be determined at each time step or each event during the simulation with Eqs. (23) and (34), we cannot predict what the outflow share will be in steady state, and thus find the final critical exit, before simulating the whole congestion propagation in the reservoir. Finding the final outflow distribution would actually require to solve the system Eq. (11) under congested conditions with the first approach. Using Eqs. (15) and (24) leads to: $\forall i \in \{1, \dots, N\}$, $q_{in,i}(t) = n_i(t)/L_i V(n(t)) = q_{out,i}(t) = \frac{n_i(t)}{n(t)} \frac{L(t)}{L_i} \mu(t)$, thus $n(t)/L(t)V(n(t)) = \mu(t)$, but this is insufficient to get the final solution. Actually, solving analytically this system seems intractable as the equilibrium state in congestion depends also on the demands $\lambda_i(t)$. This is shown in Fig. A.1(a), where the outflow ratio $q_{out,2}/q_{out,1}$ in steady state is displayed for different simulation runs. We observe that a high demand on a route does not necessarily imply a high outflow on this route. This is because the outflow ratio also depends on the trip lengths, namely a high demand on a long route often results in a low outflow compared to the short route. Actually, four different cases of outflow share can be exhibited out of these results, as presented in Fig. A.1(b):

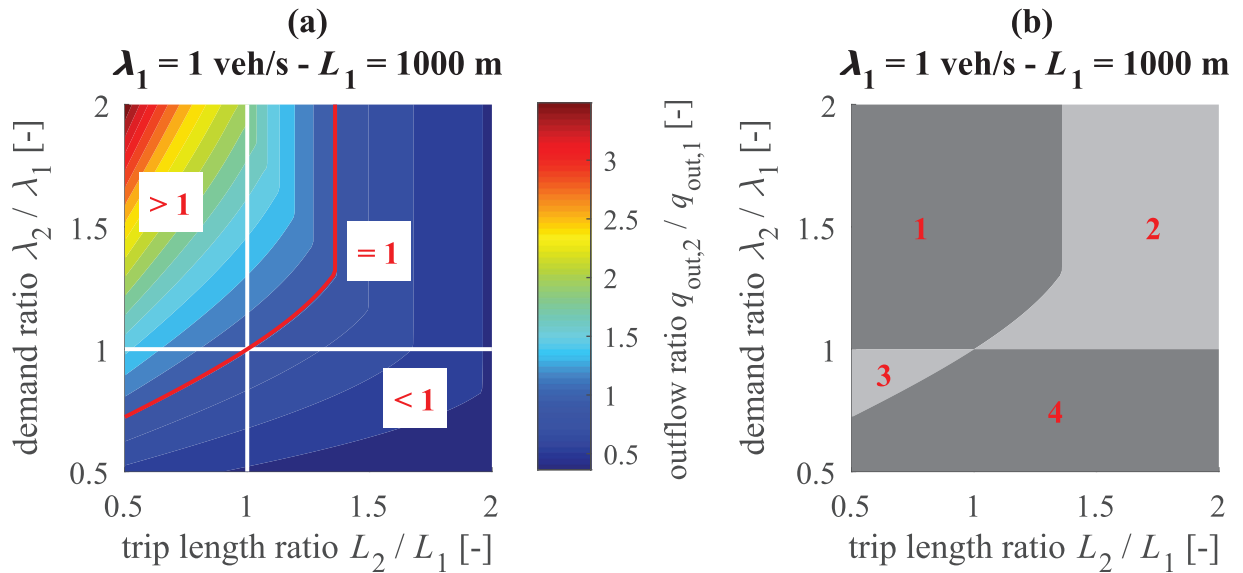


Fig. A.1. (a) Outflow ratio $q_{out,2}/q_{out,1}$ in steady state for different simulations with different trip length L_2/L_1 and demand λ_2/λ_1 ratios, (b) four areas in the same graph delimiting different steady state cases.

- Case 1: intuitive, $\lambda_1 < \lambda_2$ gives $q_{out,1} < q_{out,2}$
- Case 2: less intuitive, $\lambda_1 < \lambda_2$ gives $q_{out,1} > q_{out,2}$
- Case 3: less intuitive, $\lambda_1 > \lambda_2$ gives $q_{out,1} < q_{out,2}$
- Case 4: intuitive, $\lambda_1 > \lambda_2$ gives $q_{out,1} > q_{out,2}$

Cases 1 and 4 are intuitive, as the order of flows (according to the demands) is respected in the outflow share. But cases 2 and 3 are less intuitive, as the order of flows is reversed in the outflow share. This phenomenon is due to the differences in trip lengths. Although these graphs can provide some insights about the inner dynamics of such a system, they still depend on specific values for λ_1 and L_1 , and could be hardly generalized to three or more routes.

References

- Aboudolas, K., Geroliminis, N., 2013. Perimeter and boundary flow control in multi-reservoir heterogeneous networks. *Transport. Res. Part B* 55, 265–281. doi:[10.1016/j.trb.2013.07.003](https://doi.org/10.1016/j.trb.2013.07.003).
- Ampountolas, K., Zheng, N., Geroliminis, N., 2017. Macroscopic modelling and robust control of bi-modal multi-region urban road networks. *Transport. Res. Part B* 104, 616–637. doi:[10.1016/j.trb.2017.05.007](https://doi.org/10.1016/j.trb.2017.05.007).
- Arnott, R., 2013. A bathtub model of downtown traffic congestion. *J. Urban Econ.* 76, 110–121. doi:[10.1016/j.jue.2013.01.001](https://doi.org/10.1016/j.jue.2013.01.001).
- Batista, S., Leclercq, L., Geroliminis, N., 2019. Estimation of regional trip length distributions for the calibration of the aggregated network traffic models. *Transport. Res. Part B* 122, 192–217. doi:[10.1016/j.trb.2019.02.009](https://doi.org/10.1016/j.trb.2019.02.009).
- Cao, J., Menendez, M., 2015. System dynamics of urban traffic based on its parking-related-states. *Transport. Res. Part B* 81 (3), 718–736. doi:[10.1016/j.trb.2015.07.018](https://doi.org/10.1016/j.trb.2015.07.018).
- Daganzo, C.F., 1994. The cell transmission model: a dynamic representation of highway traffic consistent with the hydrodynamic theory. *Transport. Res. Part B* 28 (4), 269–287. doi:[10.1016/0191-2615\(94\)90002-7](https://doi.org/10.1016/0191-2615(94)90002-7).
- Daganzo, C.F., 1995. The cell transmission model, part ii: network traffic. *Transport. Res. Part B* 29 (2), 79–93. doi:[10.1016/0191-2615\(94\)00022-R](https://doi.org/10.1016/0191-2615(94)00022-R).
- Daganzo, C.F., 2007. Urban gridlock: macroscopic modeling and mitigation approaches. *Transport. Res. Part B* 41 (1), 49–62.

- Daganzo, C.F., Lehe, L.J., 2015. Distance-dependent congestion pricing for downtown zones. *Transport. Res. Part B* 75, 89–99. doi:[10.1016/j.trb.2015.02.010](https://doi.org/10.1016/j.trb.2015.02.010).
- Ding, H., Guo, F., Zheng, X., Zhang, W., 2017. Traffic guidance-perimeter control coupled method for the congestion in a macro network. *Transport. Res. Part C* 81, 300–316. doi:[10.1016/j.trc.2017.06.010](https://doi.org/10.1016/j.trc.2017.06.010).
- Geroliminis, N., 2009. Dynamics of peak hour and effect of parking for congested cities. *Transportation Research Board 88th Annual Meeting*. Washington DC.
- Geroliminis, N., 2015. Cruising-for-parking in congested cities with an mfd representation. *Econ. Transport.* 4 (3), 156–165. doi:[10.1016/j.ecotra.2015.04.001](https://doi.org/10.1016/j.ecotra.2015.04.001).
- Geroliminis, N., Daganzo, C.F., 2007. Macroscopic modeling of traffic in cities. *Transportation Research Board 86th Annual Meeting*. Washington DC.
- Geroliminis, N., Daganzo, C.F., 2008. Existence of urban-scale macroscopic fundamental diagrams: some experimental findings. *Transport. Res. Part B* 42 (9), 759–770.
- Haddad, J., 2015. Robust constrained control of uncertain macroscopic fundamental diagram networks. *Transport. Res. Part C* 59, 323–339. doi:[10.1016/j.trc.2015.05.014](https://doi.org/10.1016/j.trc.2015.05.014).
- Haddad, J., Mirkin, B., 2016. Adaptive perimeter traffic control of urban road networks based on mfd model with time delays. *Int. J. Robust Nonlinear Control* 26, 1267–1285. doi:[10.1002/rnc.3502](https://doi.org/10.1002/rnc.3502).
- Haddad, J., Mirkin, B., 2017. Coordinated distributed adaptive perimeter control for large-scale urban road networks. *Transport. Res. Part C* 77, 495–515. doi:[10.1016/j.trc.2016.12.002](https://doi.org/10.1016/j.trc.2016.12.002).
- Haddad, J., Zheng, Z., 2017. Adaptive perimeter control with state delays in two urban regions. In: *Transportation Research Board 96th Annual Meeting*, p. 18p. Washington DC.
- Hajiahmadi, M., Knoop, V., De Schutter, B., Hellendoorn, H., 2013. Optimal dynamic route guidance: a model predictive approach using the macroscopic fundamental diagram. In: *Intelligent Transportation Systems - (ITSC), 2013 16th International IEEE Conference on*, pp. 1022–1028. doi:[10.1109/ITSC.2013.6728366](https://doi.org/10.1109/ITSC.2013.6728366).
- Jin, W., Zhang, H., 2003. On the distribution schemes for determining flows through a merge. *Transport. Res. Part B* 37 (6), 521–540. doi:[10.1016/S0191-2615\(02\)00026-7](https://doi.org/10.1016/S0191-2615(02)00026-7).
- Keyvan-Ekbatani, M., Kouvelas, A., Papamichail, I., Papageorgiou, M., 2012. Exploiting the fundamental diagram of urban networks for feedback-based gating. *Transport. Res. Part B* 46 (10), 1393–1403. doi:[10.1016/j.trb.2012.06.008](https://doi.org/10.1016/j.trb.2012.06.008).
- Knoop, V.L., Hoogendoorn, S.P., 2014. Network transmission model: a dynamic traffic model at network level. *Transportation Research Board 93rd Annual Meeting*. Washington DC.
- Kouvelas, A., Saeedmanesh, M., Geroliminis, N., 2017. Enhancing model-based feedback perimeter control with data-driven online adaptive optimization. *Transport. Res. Part B* 96, 26–45. doi:[10.1016/j.trb.2016.10.011](https://doi.org/10.1016/j.trb.2016.10.011).
- Lamotte, R., Geroliminis, N., 2018. The morning commute in urban areas with heterogeneous trip lengths. *Transport. Res. Part B* 117, 794–810. doi:[10.1016/j.trb.2017.08.023](https://doi.org/10.1016/j.trb.2017.08.023).
- Laval, J.A., Leclercq, L., Chiabaut, N., 2018. Minimal parameter formulations of the dynamic user equilibrium using macroscopic urban models: freeway vs city streets revisited. *Transport. Res. Part B* 117, 676–686. doi:[10.1016/j.trb.2017.08.027](https://doi.org/10.1016/j.trb.2017.08.027).
- Leclercq, L., Becarie, C., 2012. Meso Lighthill-Whitham and richards model designed for network applications. *Transportation Research Board 91st Annual Meeting*. Washington DC.
- Leclercq, L., Parzani, C., Knoop, V.L., Amourette, J., Hoogendoorn, S.P., 2015. Macroscopic traffic dynamics with heterogeneous route patterns. *Transport. Res. Part C* 55, 292–307. doi:[10.1016/j.trc.2015.05.006](https://doi.org/10.1016/j.trc.2015.05.006).
- Leclercq, L., Sénécat, A., Mariotte, G., 2017. Dynamic macroscopic simulation of on-street parking search: a trip-based approach. *Transport. Res. Part B* 101, 268–282. doi:[10.1016/j.trb.2017.04.004](https://doi.org/10.1016/j.trb.2017.04.004).
- Lentzakis, A.F., Ware, S.I., Su, R., 2016. Region-based dynamic forecast routing for autonomous vehicles. In: *2016 IEEE 19th International Conference on Intelligent Transportation Systems (ITSC)*, pp. 1464–1469. doi:[10.1109/ITSC.2016.7795750](https://doi.org/10.1109/ITSC.2016.7795750).
- Little, J.D.C., 1961. A proof for the queuing formula. *Oper. Res.* 9 (3), 383–387.
- Mariotte, G., Leclercq, L., Laval, J.A., 2017. Macroscopic urban dynamics: analytical and numerical comparisons of existing models. *Transport. Res. Part B* 101, 245–267. doi:[10.1016/j.trb.2017.04.002](https://doi.org/10.1016/j.trb.2017.04.002).
- Newell, G.F., 1993. A simplified theory of kinematic waves in highway traffic, part ii: queuing at freeway bottlenecks. *Transport. Res. Part B* 27 (4), 289–303. doi:[10.1016/0191-2615\(93\)90039-D](https://doi.org/10.1016/0191-2615(93)90039-D).
- Ramezani, M., Haddad, J., Geroliminis, N., 2015. Dynamics of heterogeneity in urban networks: aggregated traffic modeling and hierarchical control. *Transport. Res. Part B* 74, 1–19. doi:[10.1016/j.trb.2014.12.010](https://doi.org/10.1016/j.trb.2014.12.010).
- Sirmatel, I.I., Geroliminis, N., 2017. Economic model predictive control of large-scale urban road networks via perimeter control and regional route guidance. *IEEE Trans. Intell. Transp. Syst.* 19 (4), 1112–1121. doi:[10.1109/TITS.2017.2716541](https://doi.org/10.1109/TITS.2017.2716541).
- Yildirimoglu, M., Geroliminis, N., 2014. Approximating dynamic equilibrium conditions with macroscopic fundamental diagrams. *Transport. Res. Part B* 70, 186–200. doi:[10.1016/j.trb.2014.09.002](https://doi.org/10.1016/j.trb.2014.09.002).
- Yildirimoglu, M., Ramezani, M., Geroliminis, N., 2015. Equilibrium analysis and route guidance in large-scale networks with mfd dynamics. *Transport. Res. Part C* 59, 404–420. doi:[10.1016/j.trc.2015.05.009](https://doi.org/10.1016/j.trc.2015.05.009).
- Yildirimoglu, M., Sirmatel, I.I., Geroliminis, N., 2018. Hierarchical control of heterogeneous large-scale urban road networks via path assignment and regional route guidance. *Transport. Res. Part B* 118, 106–123. doi:[10.1016/j.trb.2018.10.007](https://doi.org/10.1016/j.trb.2018.10.007).
- Zheng, N., Geroliminis, N., 2016. Modeling and optimization of multimodal urban networks with limited parking and dynamic pricing. *Transport. Res. Part B* 83, 36–58. doi:[10.1016/j.trb.2015.10.008](https://doi.org/10.1016/j.trb.2015.10.008).